

Micro- and Nanoscale Mechanical Testing

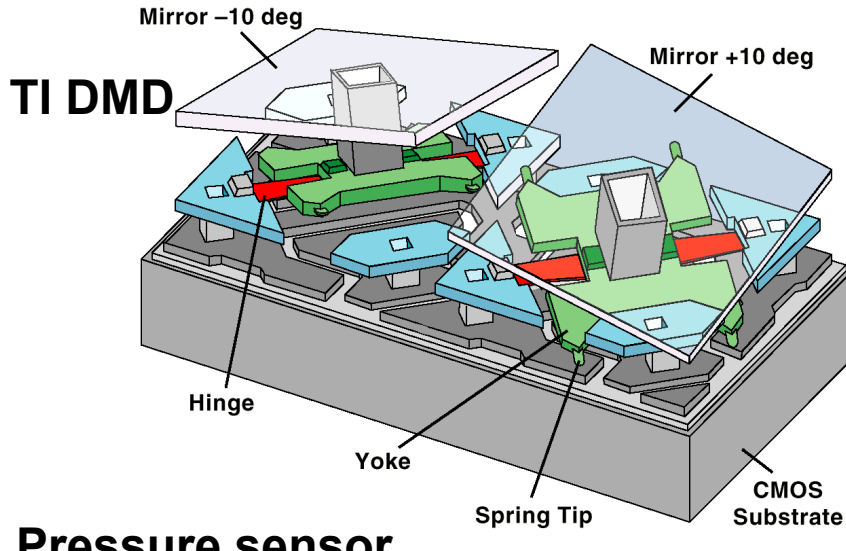
Maarten P. de Boer
MEMS Technologies Dept.
Sandia National Laboratories,
Albuquerque, NM, 87185

**Sandia is a multiprogram laboratory operated by Sandia Corporation, a
Lockheed Martin Company, for the United States Department of Energy
under contract DE-AC04-94AL85000.**

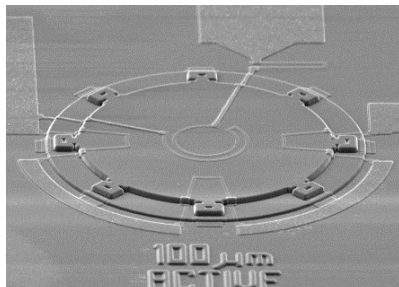


With MEMS we can accomplish electromechanical and optical functions

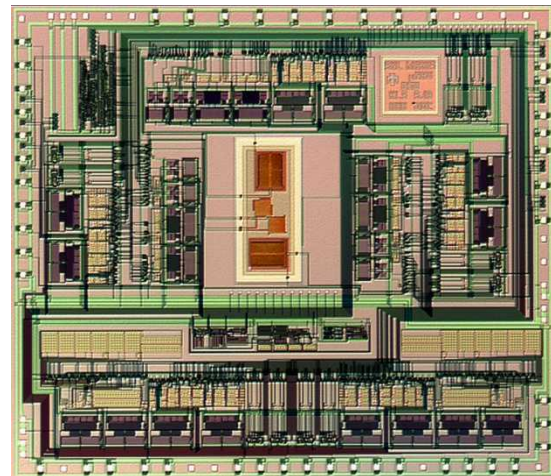
- thousands of devices simultaneously
- no assembly required
- hundreds of device concepts explored



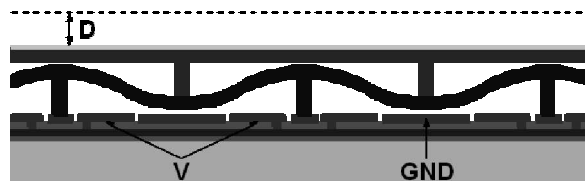
Pressure sensor



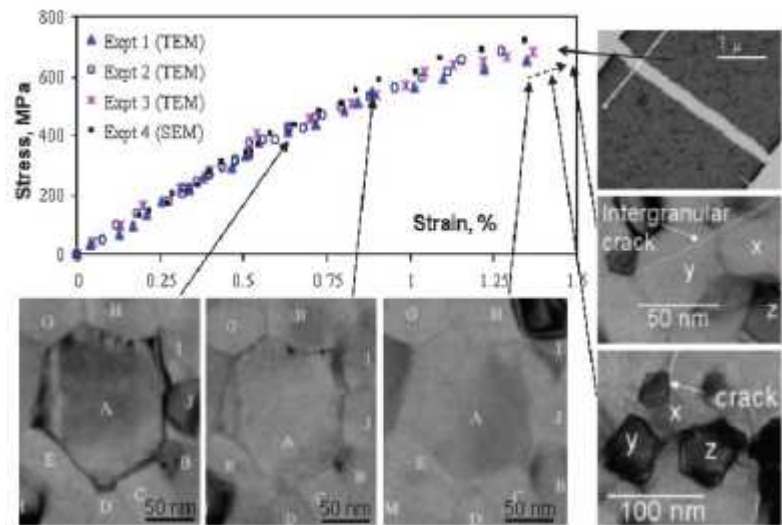
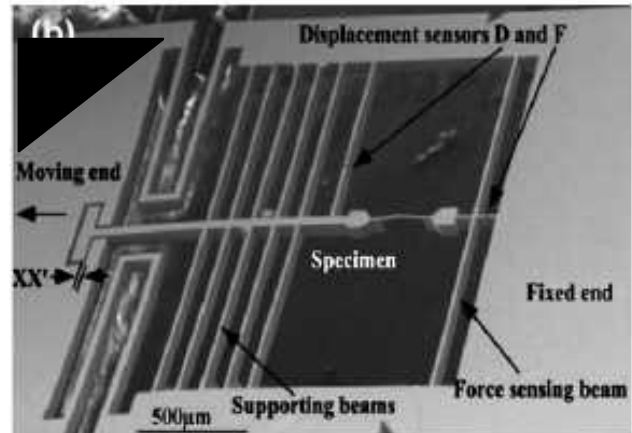
Integrated inertial sensor



Polychromator :
programmable
diffraction grating

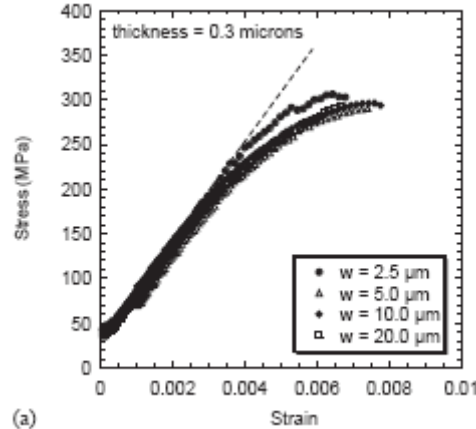
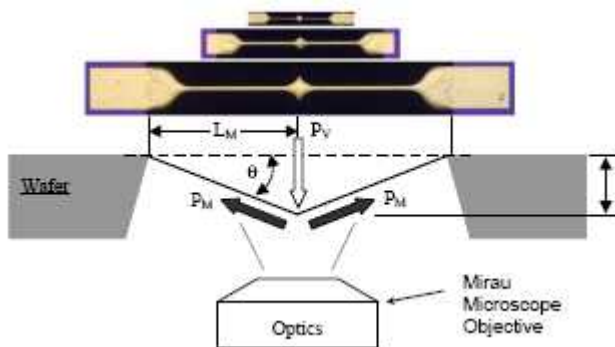


Many methods for micro and nanoscale mechanical testing are being developed



In-situ TEM

Haque and Saif (PNAS, 2004)



Membrane Deflection
Espinosa et al. (JMPS, 2004)

Consider a prototypical MEMS device (μ relay) to determine important mechanical properties

IEEE MICROWAVE AND GUIDED WAVE LETTERS, VOL. 8, NO. 8, AUGUST 1998

Performance of Low-Loss RF MEMS Capacitive Switches

Charles L. Goldsmith, *Senior Member, IEEE*, Zhimin Yao, *Member, IEEE*,
Susan Eshelman, *Member, IEEE*, and David Denniston, *Member, IEEE*

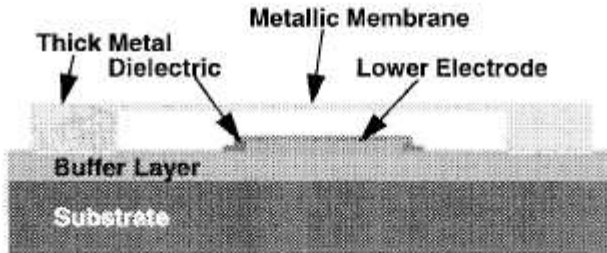


Fig. 1. Cross section of an RF MEMS capacitive switch.

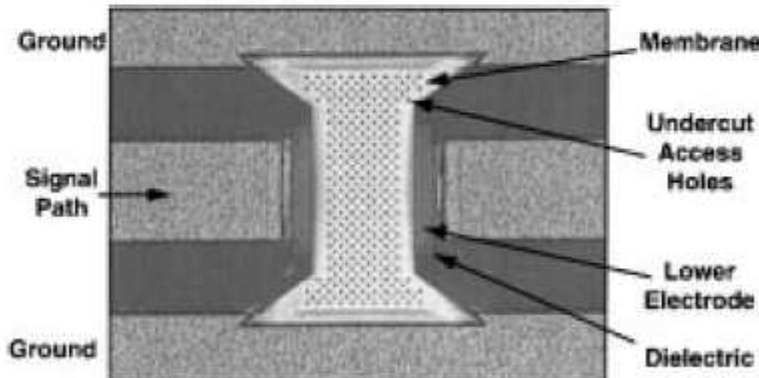


Fig. 2. Top view of a shunt MEMS capacitive switch.

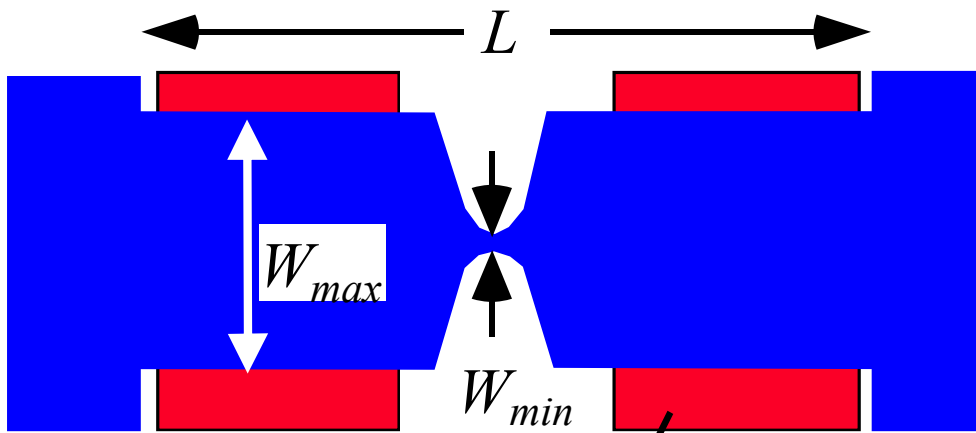
Important characteristics:

- 1) Speed
- 2) Low Voltage
- 3) Large pull-off force
- 4) No change in performance

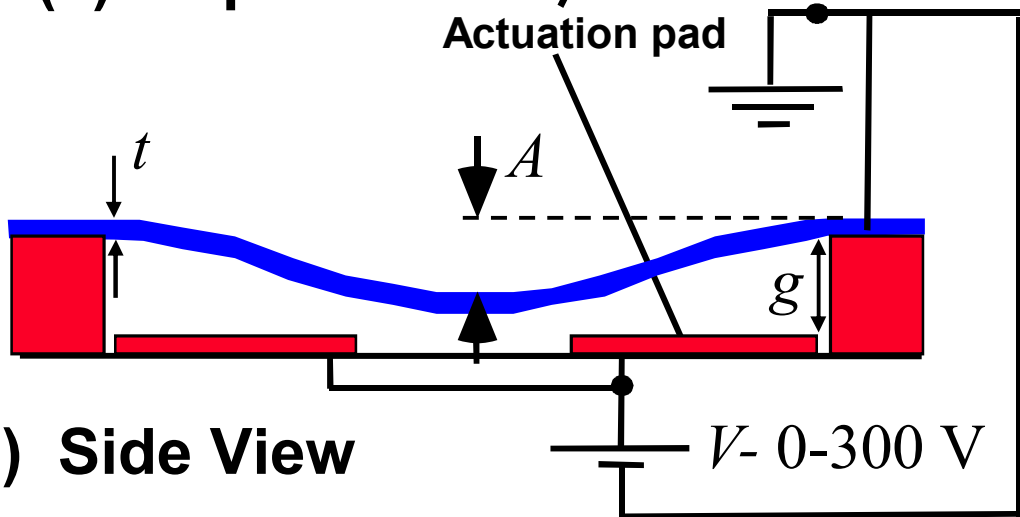
Performance depends on these mechanical properties:

- 1) E (Young's Modulus)
- 2) σ_R (residual stress)
- 3) σ_Y (yield strength)
- 4) σ_F (fatigue strength)
- 5) σ_C (creep limit)

Propose a notched, fixed-fixed beam structure to study the mechanical limits



(a) Top View



Advantages:

electrostatic actuation:

- contactless
- high cycles
- sample handling easy
- automatic testing possible

mechanical force amplification
→ small area ($500 \mu\text{m} \times 100 \mu\text{m}$)

thin films ($0.2 - 0.65 \mu\text{m}$)

Device	W_{max}	W_{min}
1	$50 \mu\text{m}$	$2.2 \mu\text{m}$
2	50	8.2
3	50	18.2

MEMS – surface micromachining implementation

A series of structural and sacrificial layers are deposited

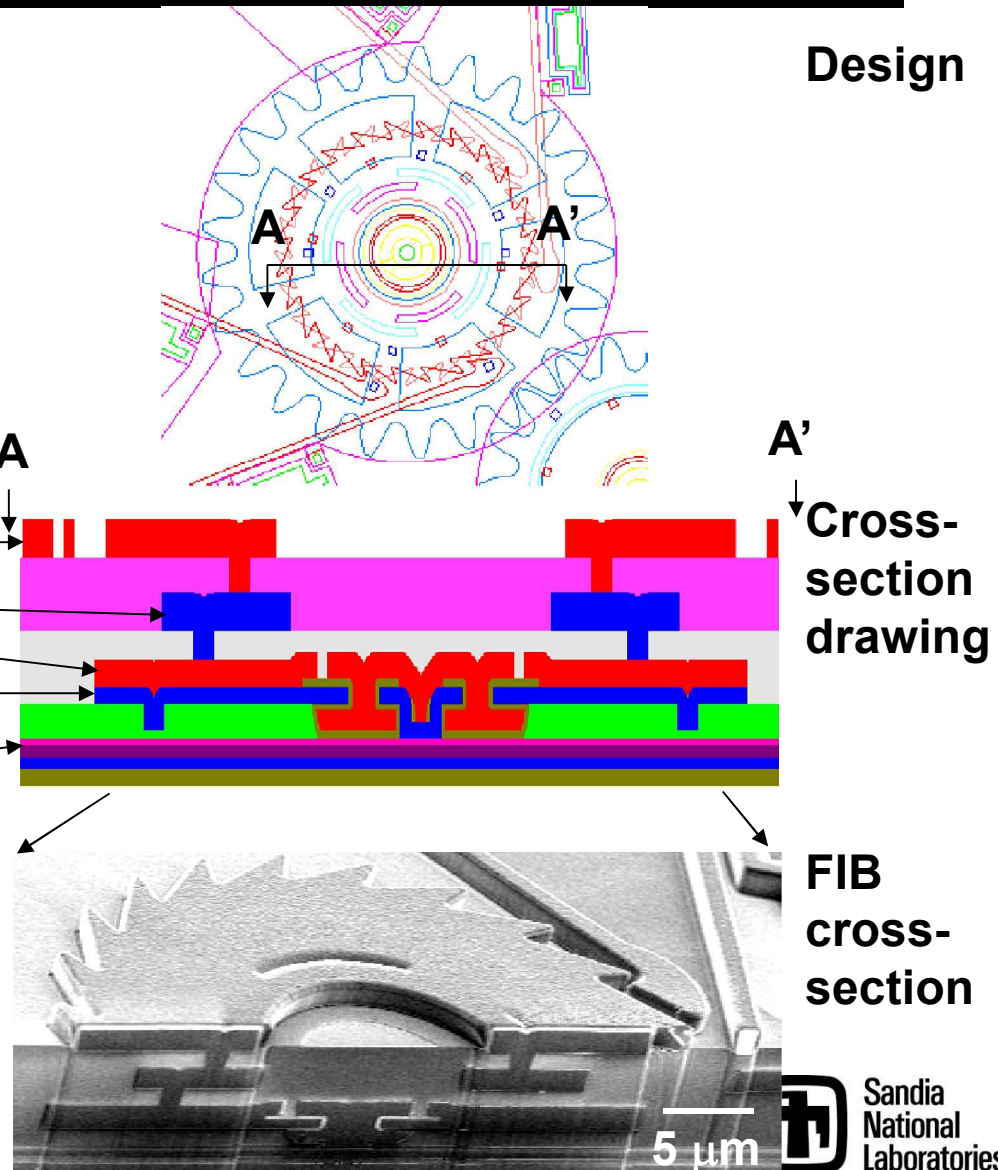
Ground plane layer (Poly 0)
4 structural levels
(Poly 1 - Poly 4)

Chemical Mechanical
Planarization (CMP)

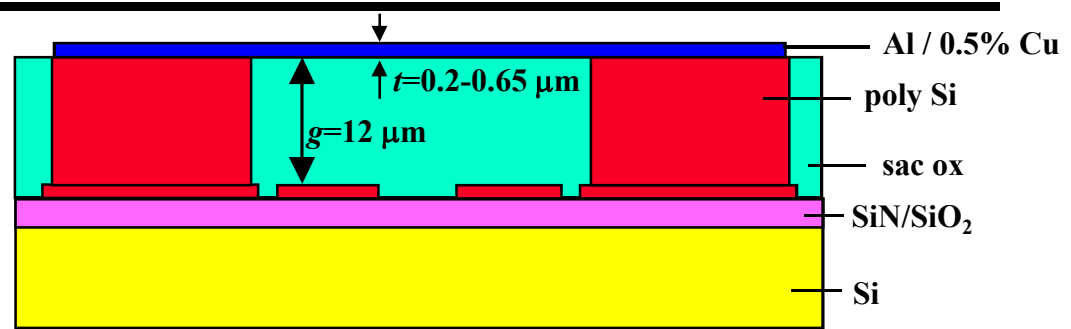
1 μm design rule

Create freestanding thin film
structures by “release”
process

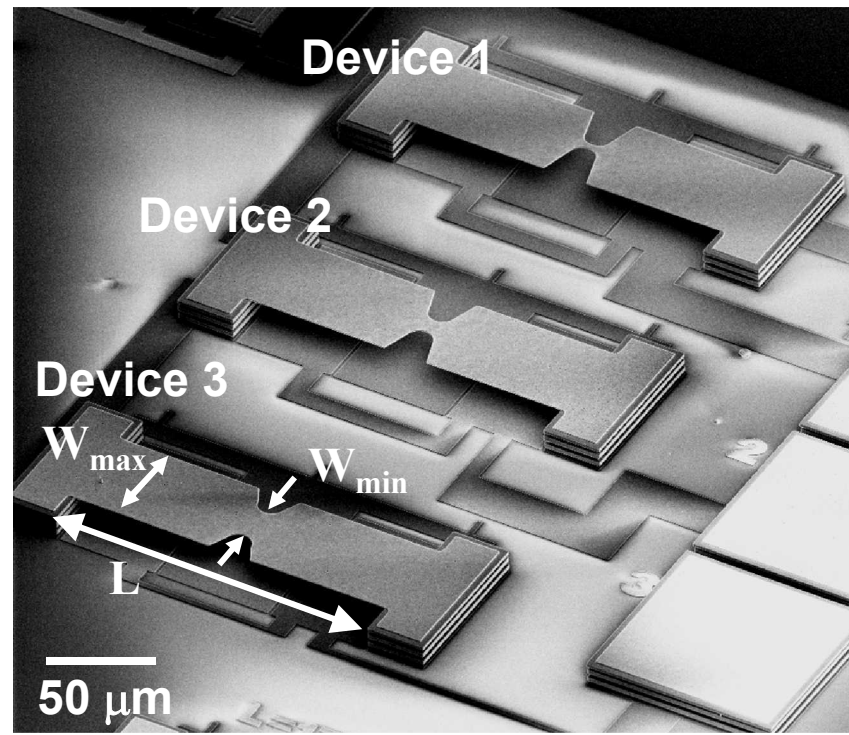
Sniegowski & de Boer,
Annu. Rev. Mater. Sci.
(2000)



Sample Fabrication

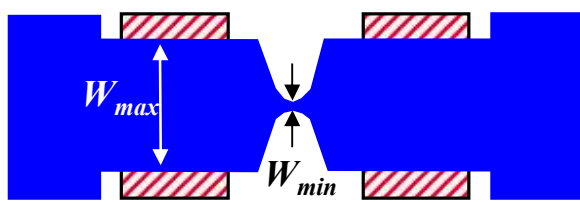
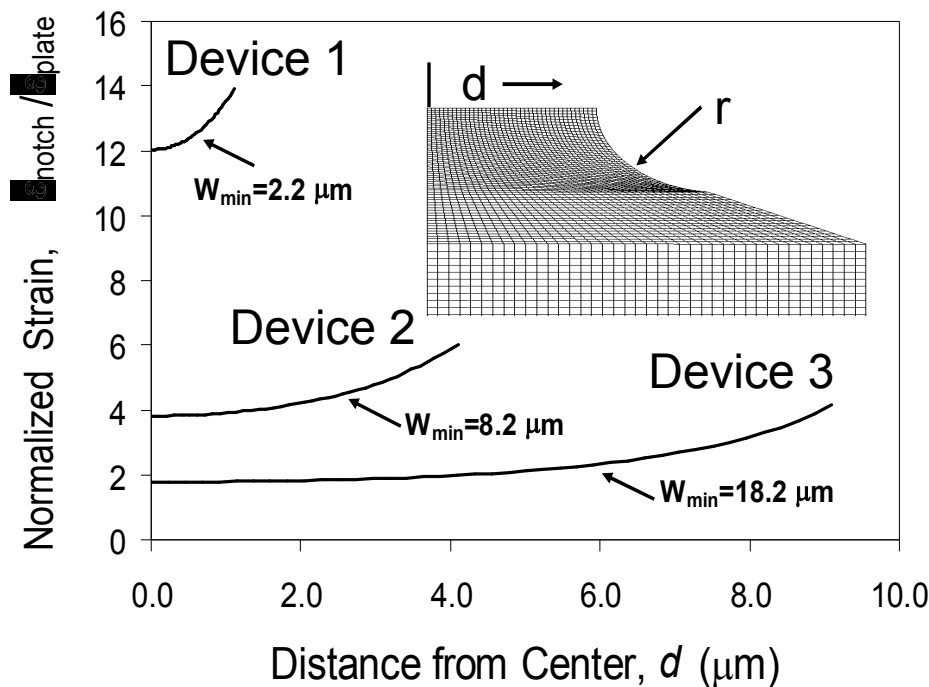


SEM
($L=160 \mu\text{m}$, $W_{\min}=18.2, 8.2, 2.2 \mu\text{m}$)

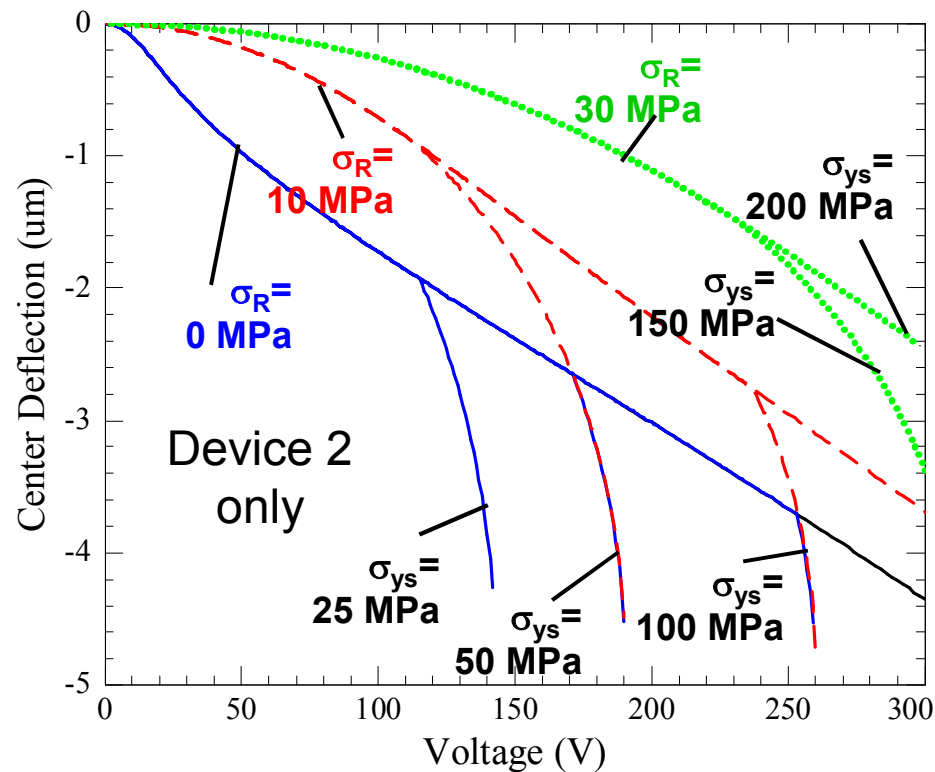


Mechanics simulations

Stress concentration due to residual or applied stress (2-D FEM)

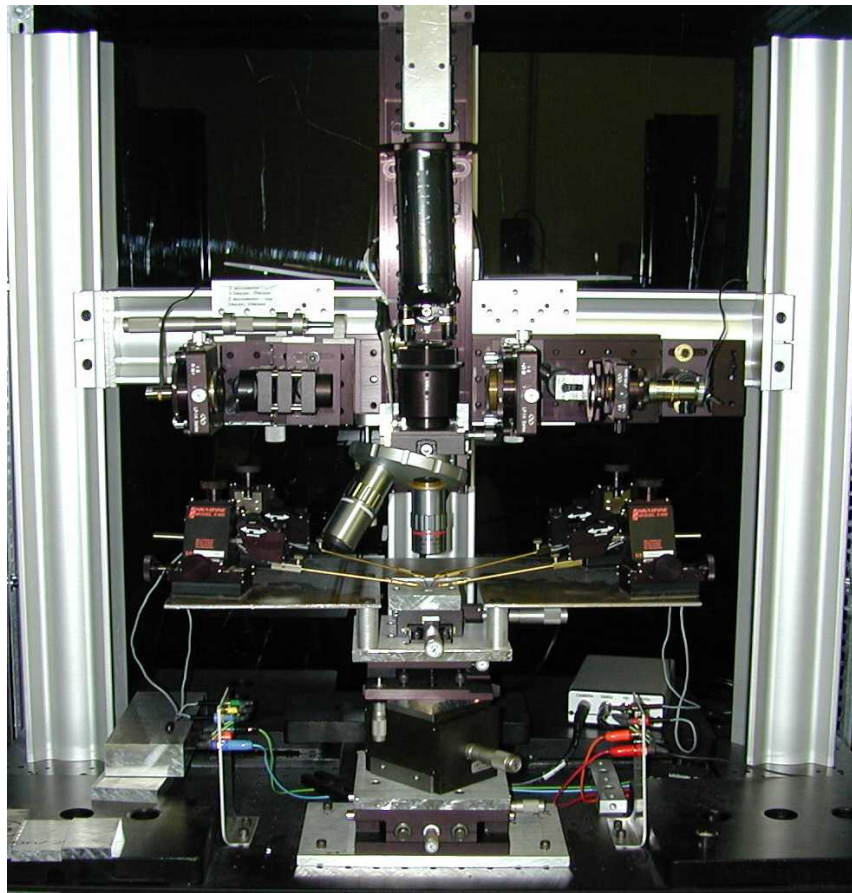


Elastic-plastic behavior in the presence of applied electrostatic load (quasi 3-D model)



De Boer et al., Part I (Acta Mater. 2008)

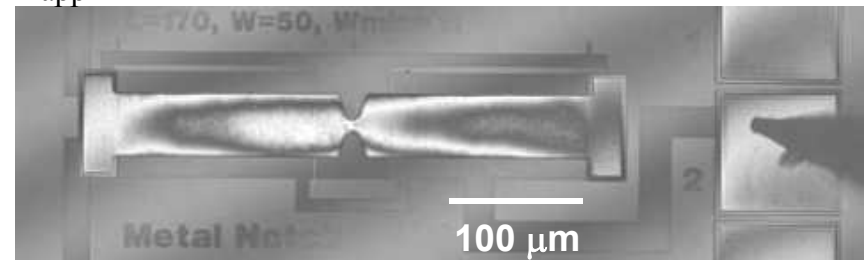
High-Resolution Probe Station (Sinclair, Corwin & de Boer, Appl. Optics, 2005)



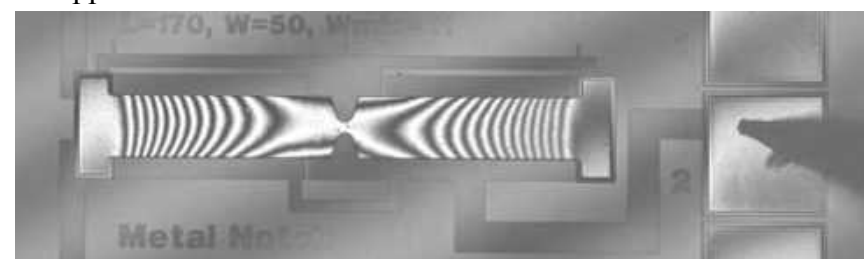
slide #9

Interferograms ($L=360 \mu\text{m}$, $W_{\min}=8.2 \mu\text{m}$)

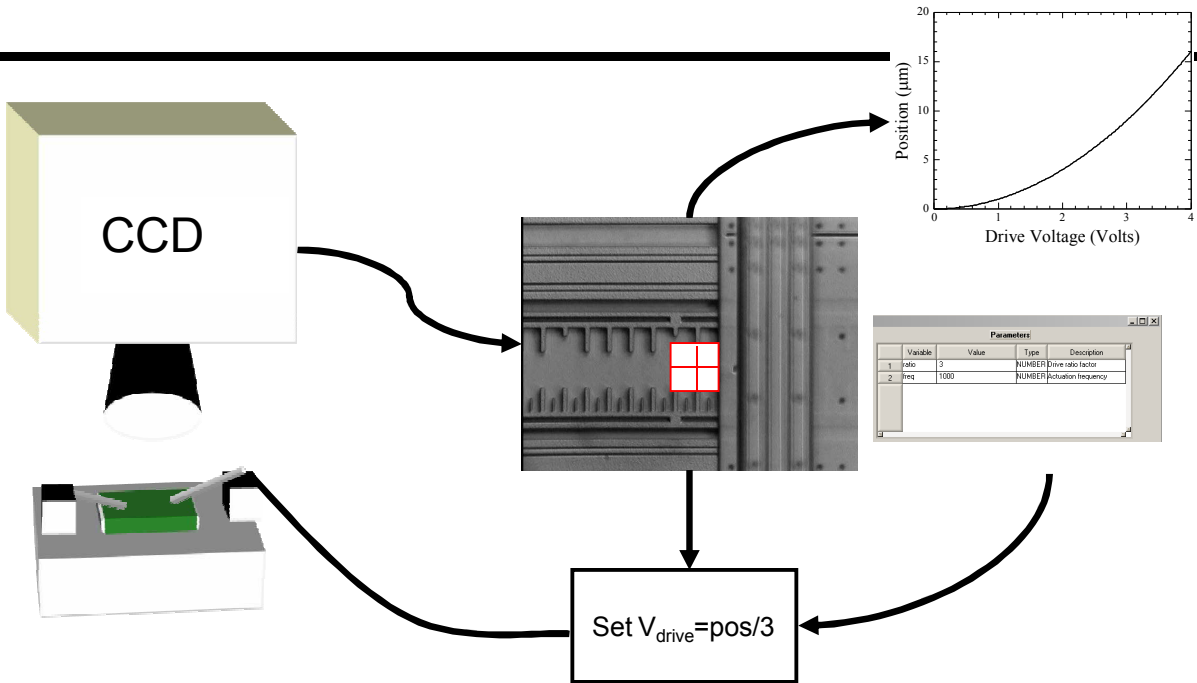
$V_{\text{app}}=0 \text{ V}$



$V_{\text{app}}=290 \text{ V}$



use phase-stepping interferometry to
measure the deflections
(full-field technique)



Intelligent Actuation: Combine real time in-plane, interferometric, and stroboscopic vision capabilities with full scripting power to allow actuation to respond to vision data in real time

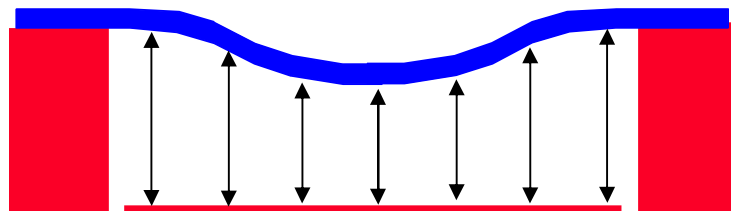
Flexibility: Works with a variety of National Instruments image capture and digital to analog boards, as well as GPIB and serial devices. Interface to external programs via DDE (i.e. LabView)

Simplicity: Presents simple user interface to allow use without knowing scripting language

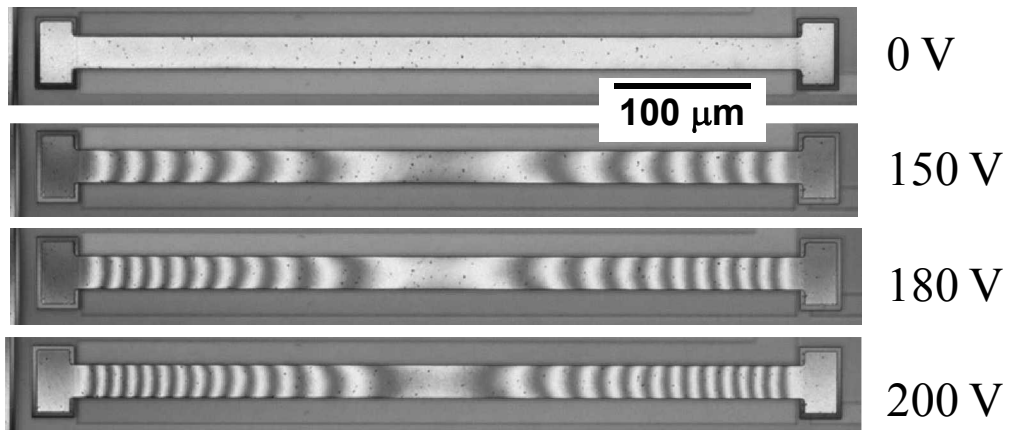
Power: Full featured scripting engine written in C includes full branching (make decisions on the fly), arithmetic function evaluation (calculate on the fly), graphing (display on the fly), file output (save data and images for further analysis/presentation)

Assess the residual stress with a fixed-fixed beam geometry

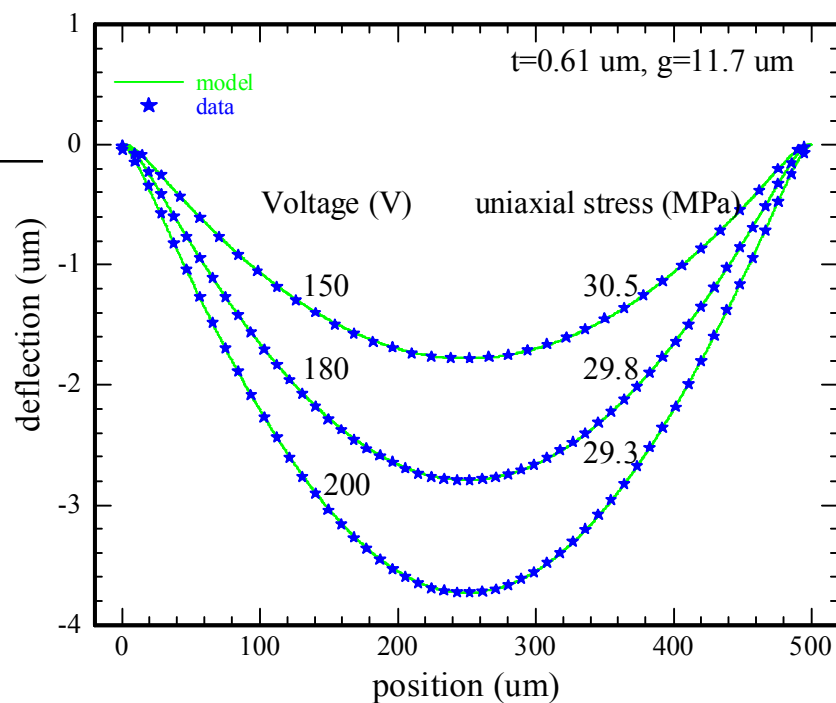
Apply electrostatic load



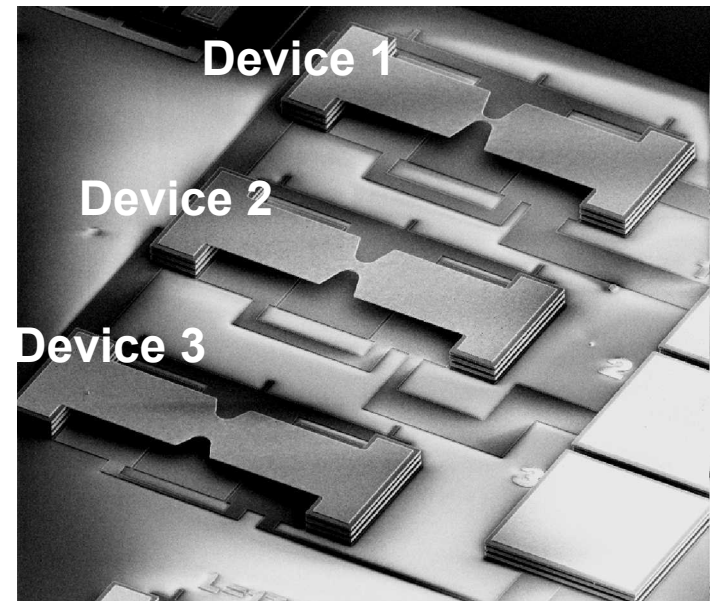
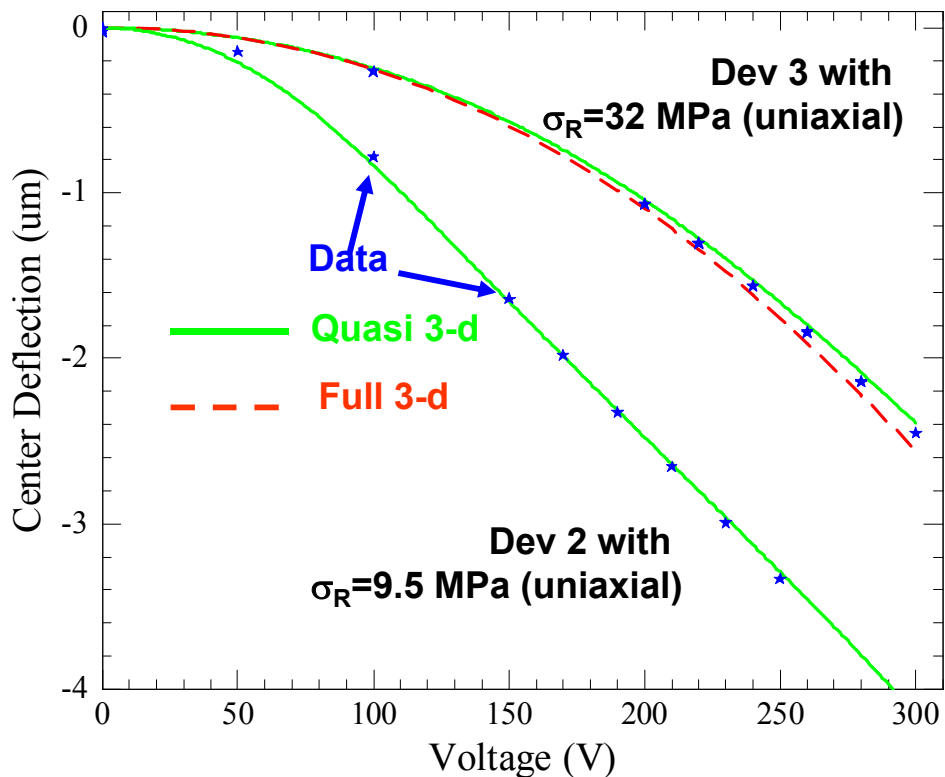
Interferograms



Measured & Modeled Deflections



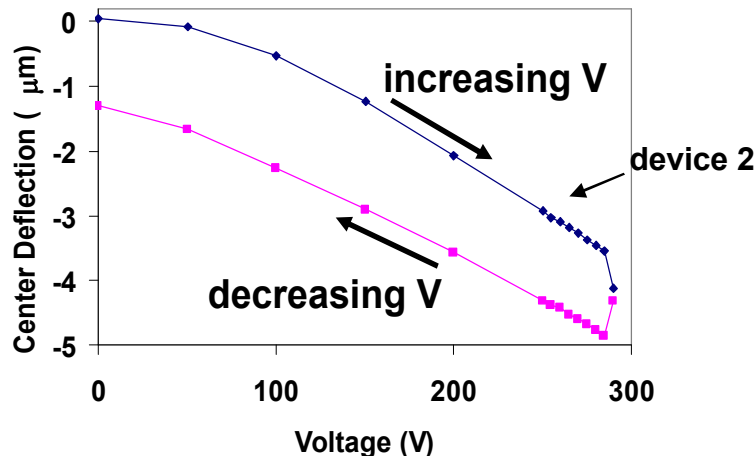
Device 3 residual stress agrees with versus ff beam, but Device 2 residual stress is lower



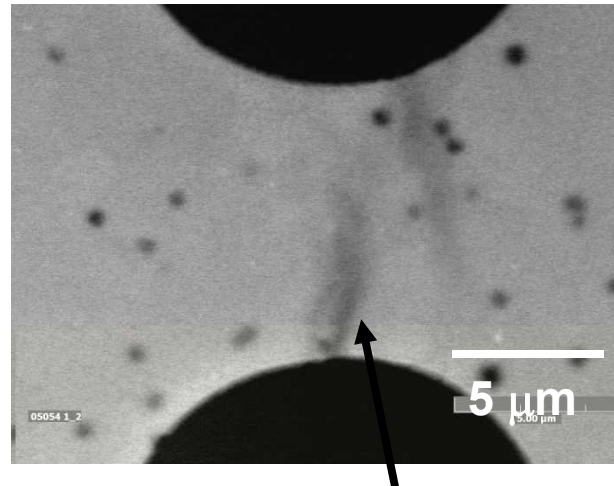
De Boer et al., Part II (Acta Mater. 2008)

Device 2 exhibits plastic behavior at slightly higher loads (290 V)

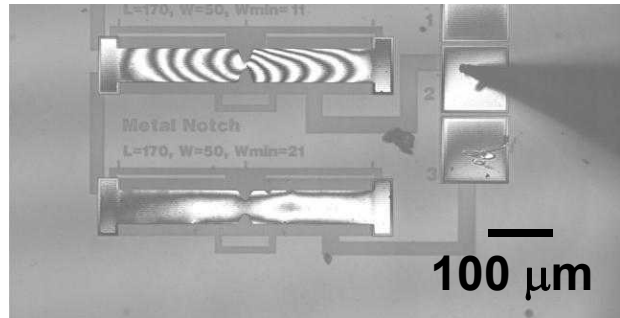
Large Hysteresis ($\sim 1.5 \mu\text{m}$)



SEM backscatter image



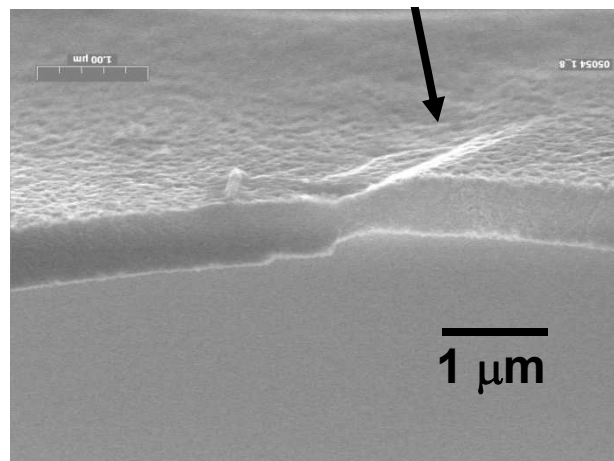
Interferogram (after actuation)



$\sigma_{ys} \sim 150 \text{ MPa}$ in heavily strained notch zone

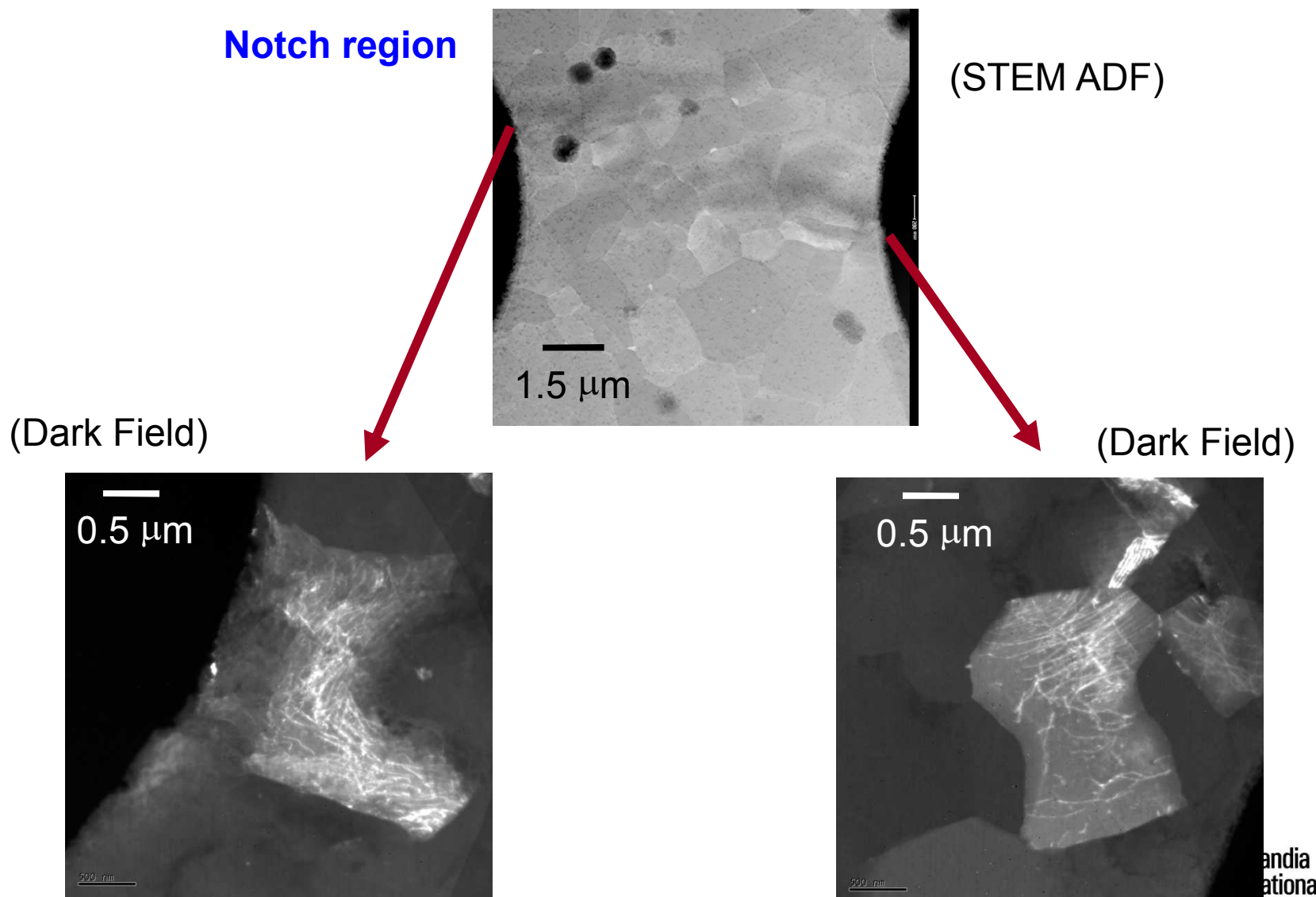
slide #13

Tilted SEM image



(r3568_r1c8)

Ex-situ TEM of plastically deformed Device 2



Device 2 fatigues

TEM: striations observed

Procedure

- 1) Fatigue for N cycles, $N=1, 10, \dots, 10^7$
 - at fixed dc voltage
 - with 10 V ac voltage modulation at 10 kHz
- 2) Apply DC voltage and measure center deflection
- 3) Repeat (1) & (2) to 10^7 cycles (20 minutes)
- 4) Choose new voltage and repeat (1)-(3)

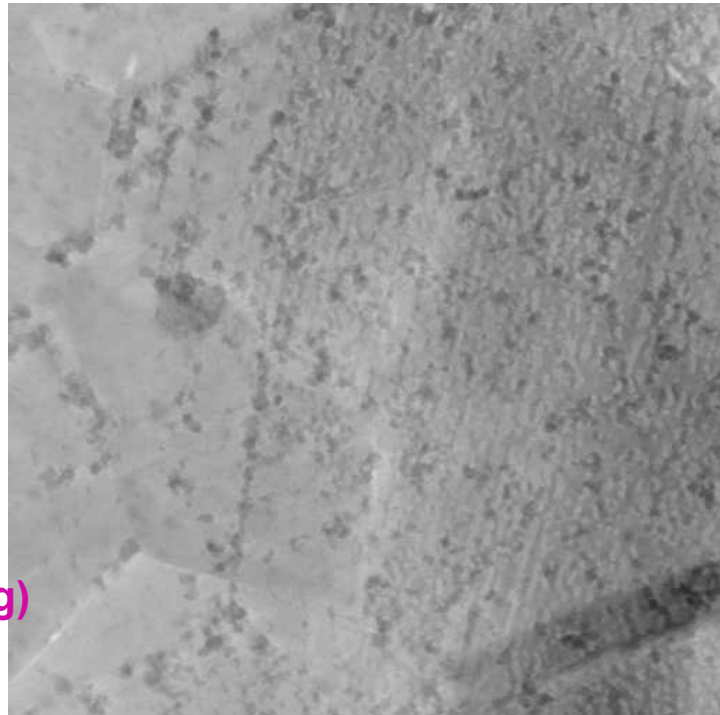
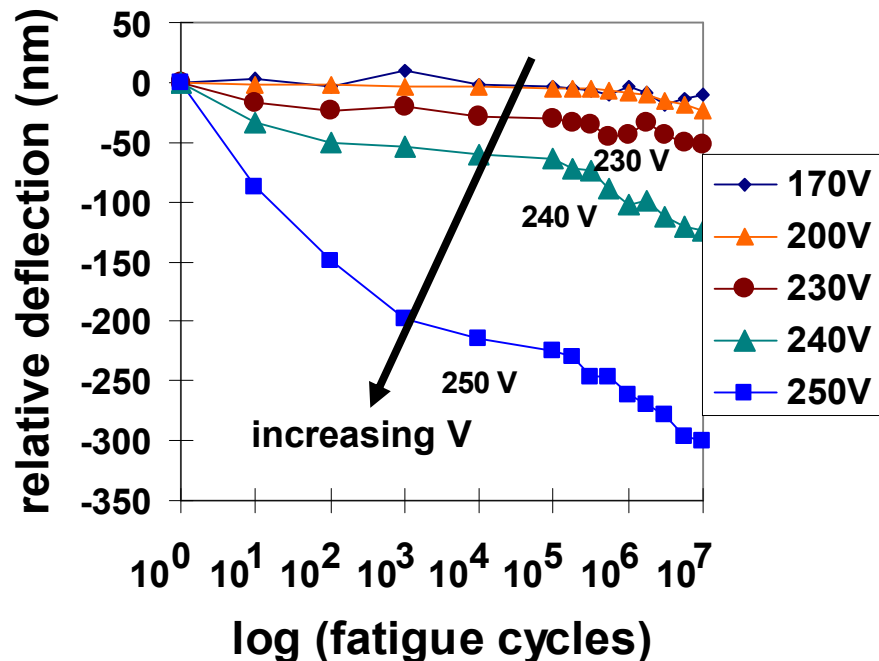
Notes:

All data on graph from one device

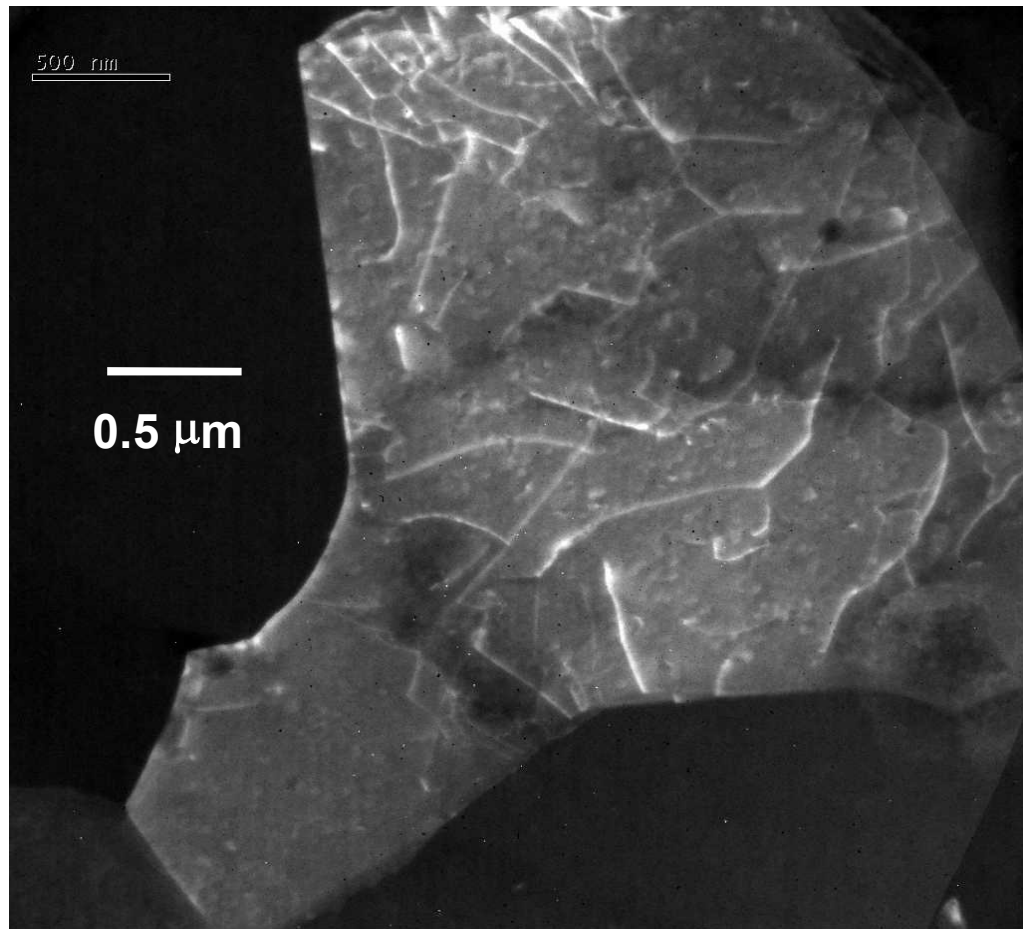
DC voltage changed randomly from test to test (not monotonically)

10 kHz modulation frequency is well below resonance

- no amplitude enhancement (stroboscopic monitoring)



Device 3 does not exhibit fatigue



Fatigued up to 10^9 cycles

No change in deflection curves

Lower bound for fatigue strength
is 172 MPa

Background dislocation density
in Device 3 sample is $\sim 10^9/\text{cm}^2$

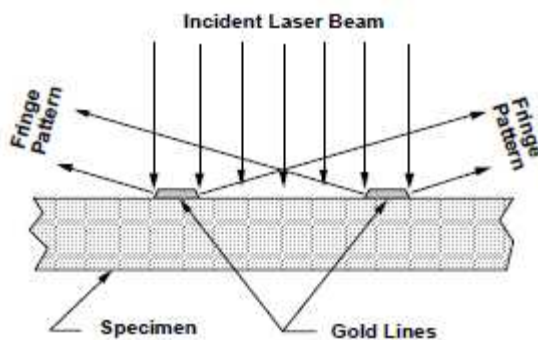
Summary – thin film metal testing

Developed an on-chip laboratory kit for easy testing of thin film metal structural materials

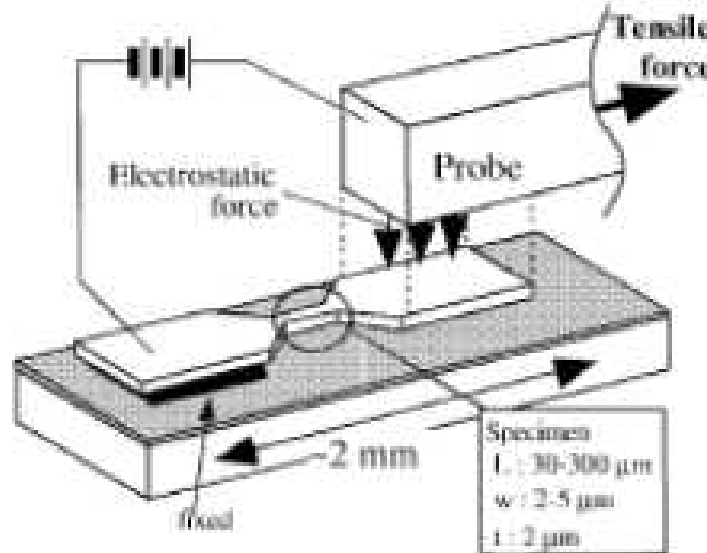
Can assess E, residual stress, strength, fatigue, (creep)

Many more experiments possible

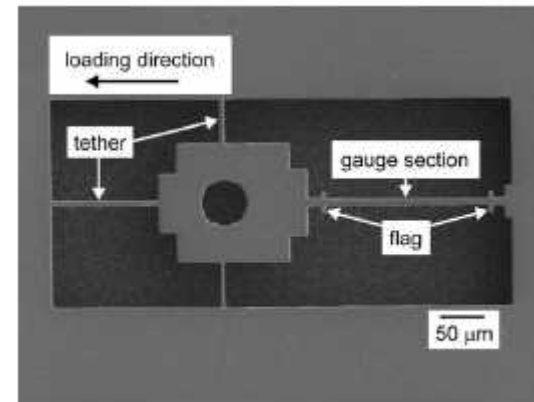
Testing of brittle materials



Sharpe
JMEMS 1996

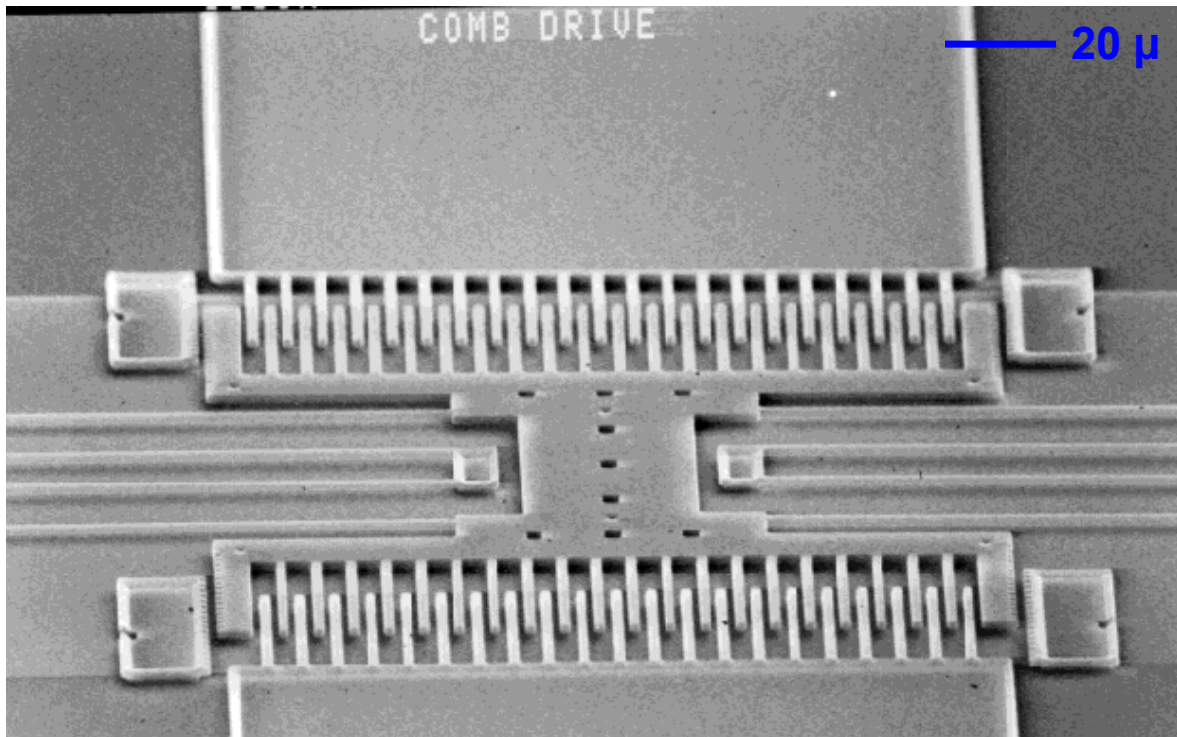


Tsuchiya
JMEMS 1996



Read and coworkers
Scripta Mat 2003

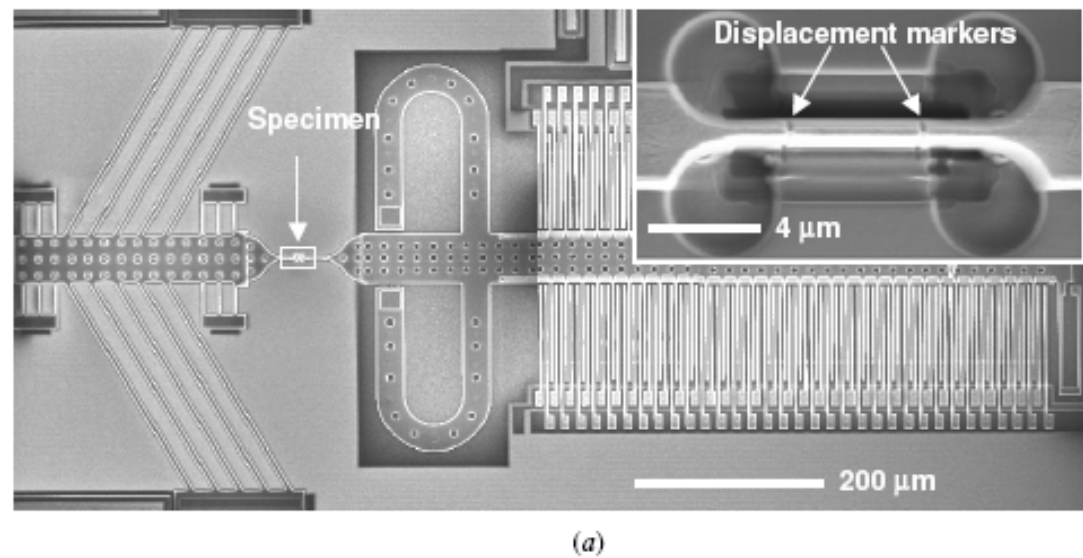
In-situ testing: How about comb drives?



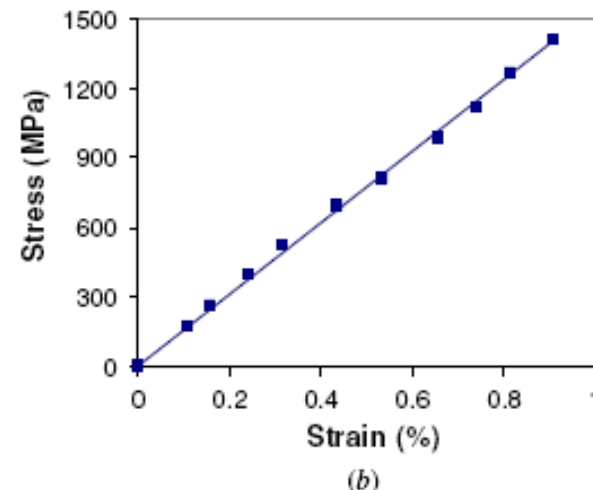
**It is Relatively Easy to Produce Motion.
It is Difficult to Perform Work!**

In-situ testing: Thermal actuators?

Zhu & Espinosa (JMM 2006)



(a)



(b)

INSTITUTE OF PHYSICS PUBLISHING
J. Microsc. Microeng. 16 (2006) 242–253

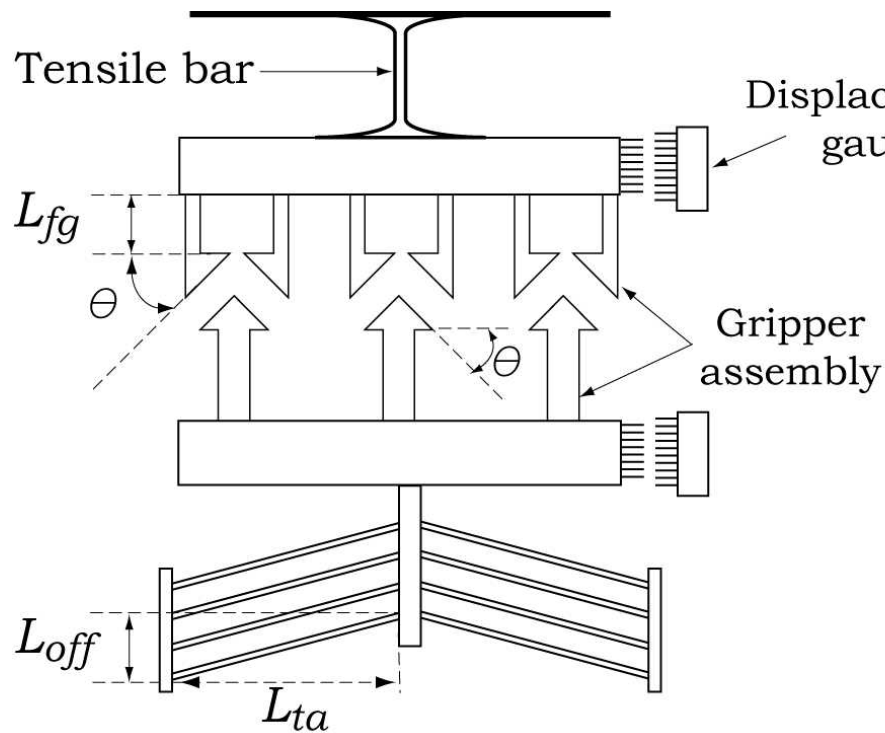
JOURNAL OF MICROMECHANICS AND MICROENGINEERING
doi:10.1088/0960-1317/16/2/008

A thermal actuator for nanoscale *in situ* microscopy testing: design and characterization

Yong Zhu, Alberto Corigliano¹ and Horacio D Espinosa

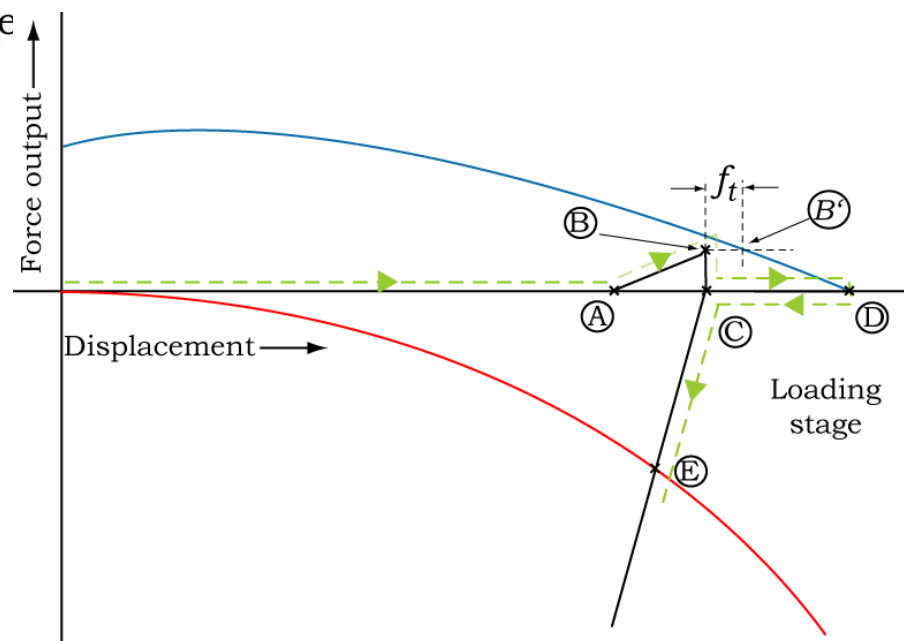
Related idea: *cooling of a thermal actuator develops large on-chip forces*

Loading schematic



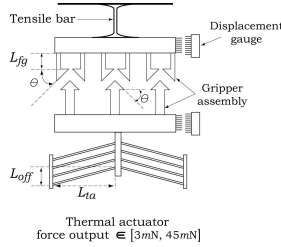
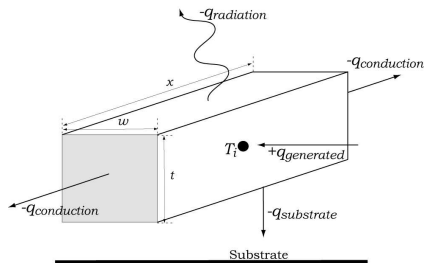
Thermal actuator
force output $\in [3mN, 45mN]$

gripper insertion: A to B
gripper engagement: D to C
tensile bar loading: C to E

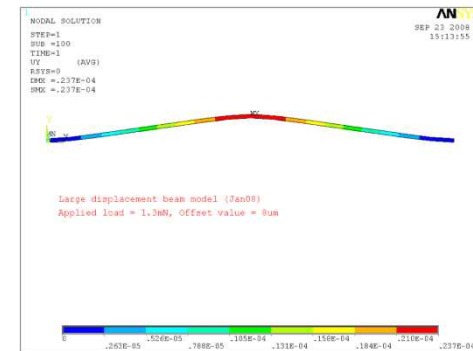


Matlab thermal model and ANSYS structural model (with some analytical calcs)

Matlab



1

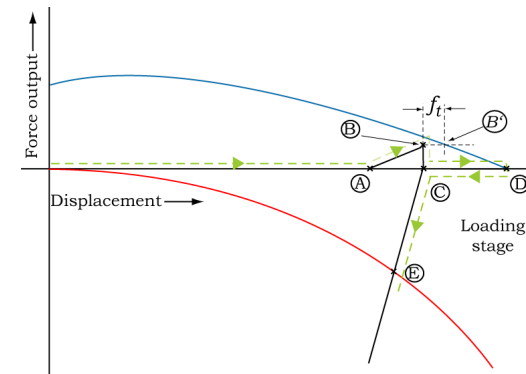
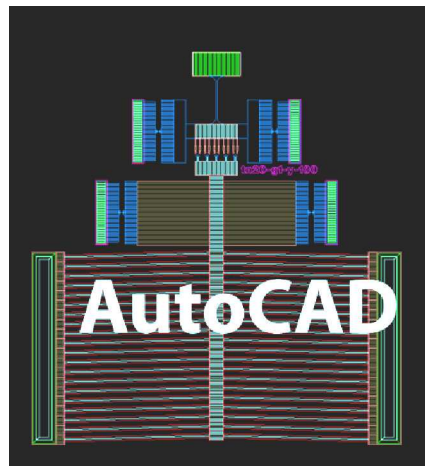


2

ANSYS

Final design

Optimization
3n



Grippers and T-bar:

Gripper geometry: $\theta=45^\circ$, $L=30 \mu\text{m}$, $W=1 \mu\text{m}$

5 pairs of grippers in each of 3 poly layers

Gripper Stiffness= 36627 N/m (analytical)

T-bar Stiffness= 7213 N/m (analytical, based on $L_{\text{Tbar}}=100 \mu\text{m}$)

Model details

Thermal Actuator:

Max Temp=600 °C

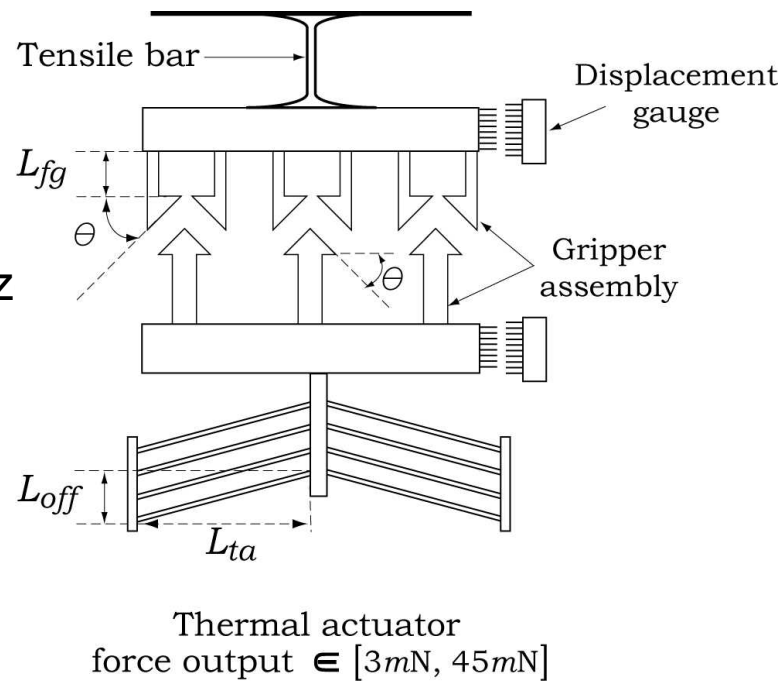
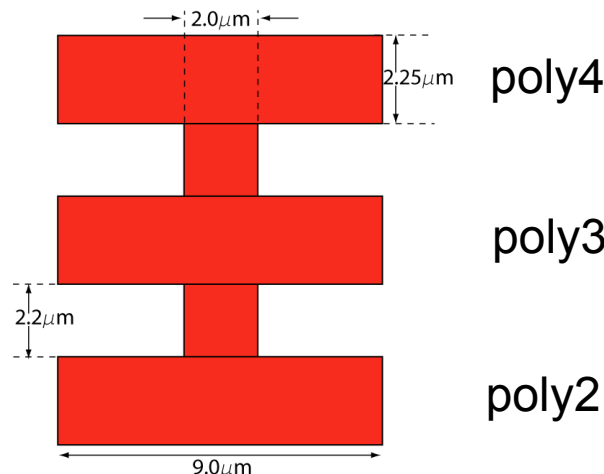
Residual stress included (15 MPa assumed)

$L_{\text{ft}}=0.5 \mu\text{m}$

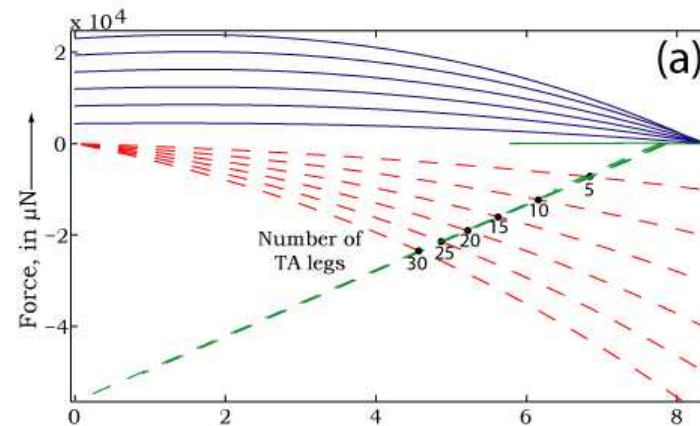
Leg length: 300 μm

Leg geometry: (make as wide as possible to maximize force, but keep $2I_{zz} < I_{xx}$ to ensure in-plane buckling)

$I_{zz}=385 \mu\text{m}^4$, $I_{xx}=852 \mu\text{m}^4$

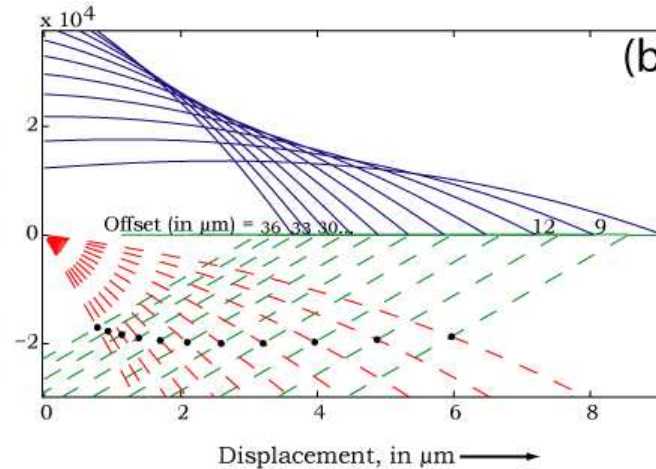


Parametric studies to optimize the design



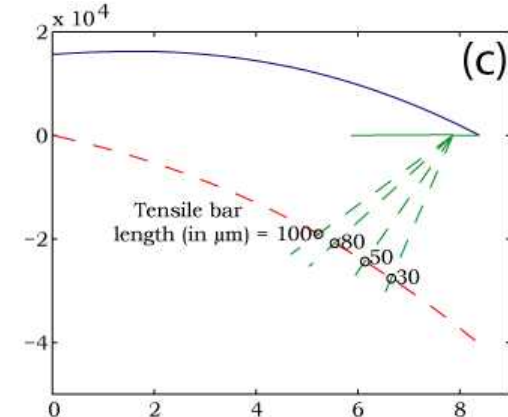
Increasing the number of TA legs increases the force. Each successive red curve is a simple superposition of the previous curve. The force increases nonlinearly because of the compliance of the tensile bar, so we want to choose an optimum number of TA legs.

Baseline: 20 legs
Range: 10-30 legs



As offset increases, max displacement decreases. But linear stretching increases, resulting in higher force at same displacement. Considering sample compliance, the net effect is small.

Baseline: 8 μm (area limit)
Range: 15, 17, 20 μm

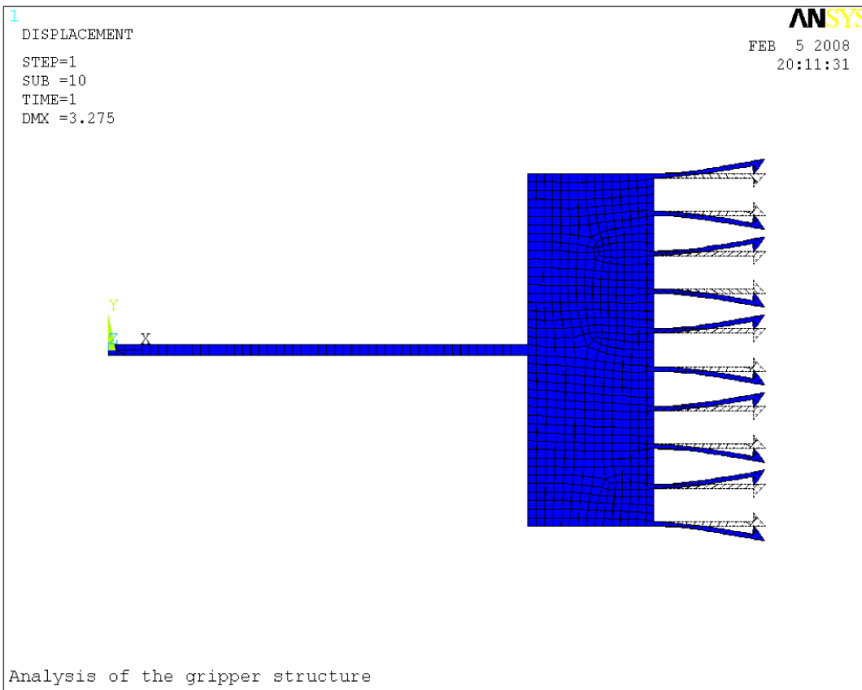


Shorter T-bar decreases compliance, resulting in higher force.

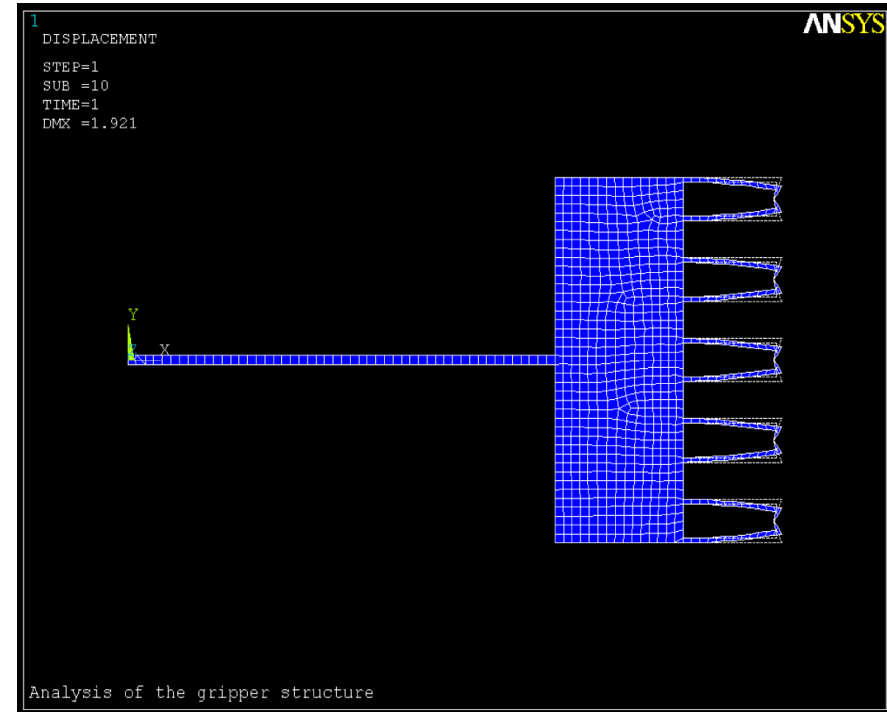
Baseline: 100 (70) μm (fillet effect)
Range: 0, 30 (16) , 100 (70) μm

ANSYS modeling of gripper insertion

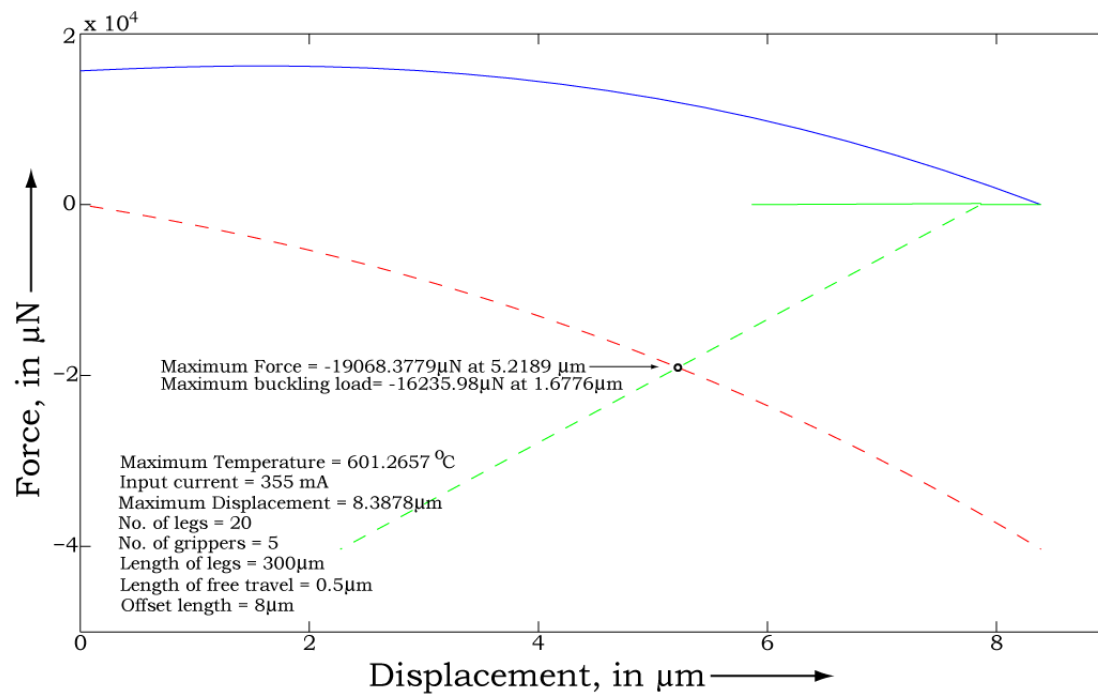
Gripper deflection



Effect of friction on grips ($\mu=0.5$, $\theta=25^\circ$)

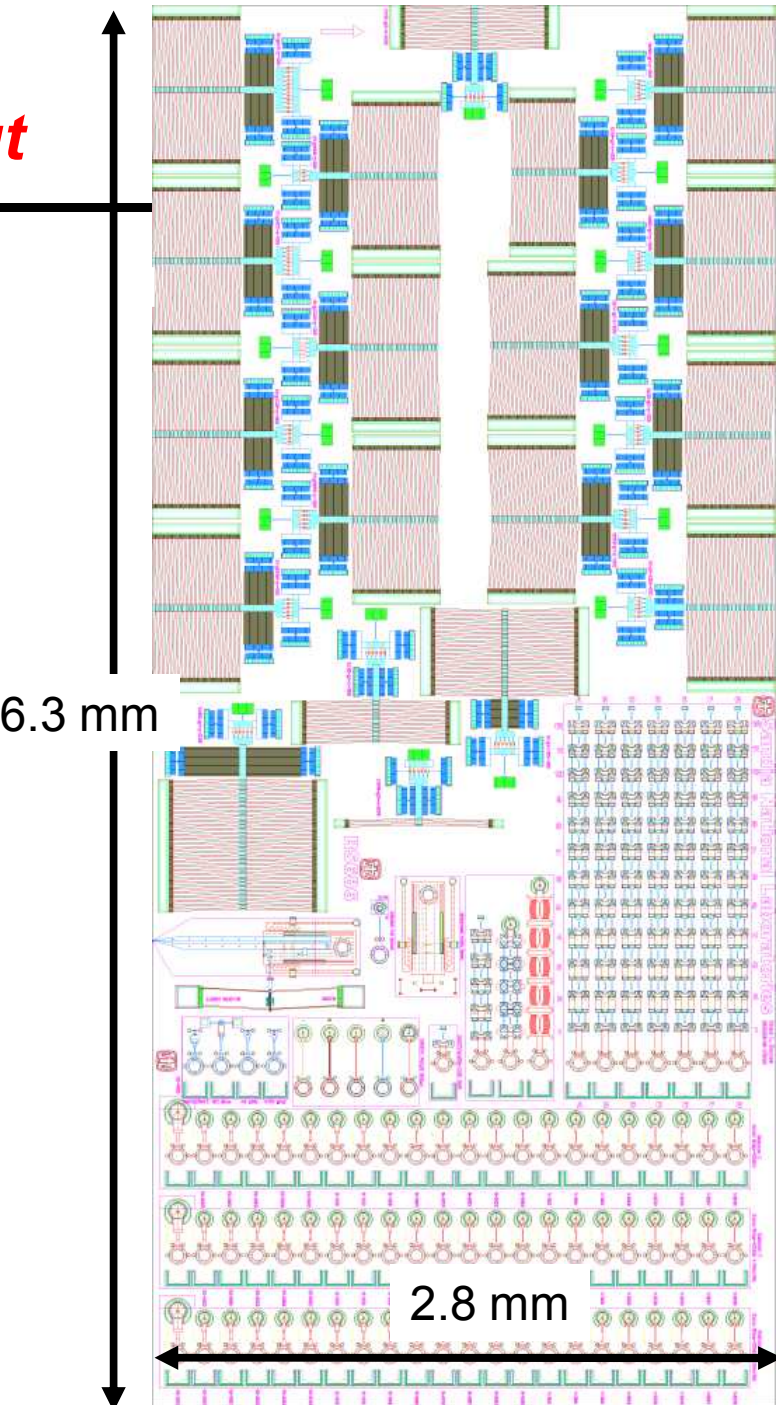
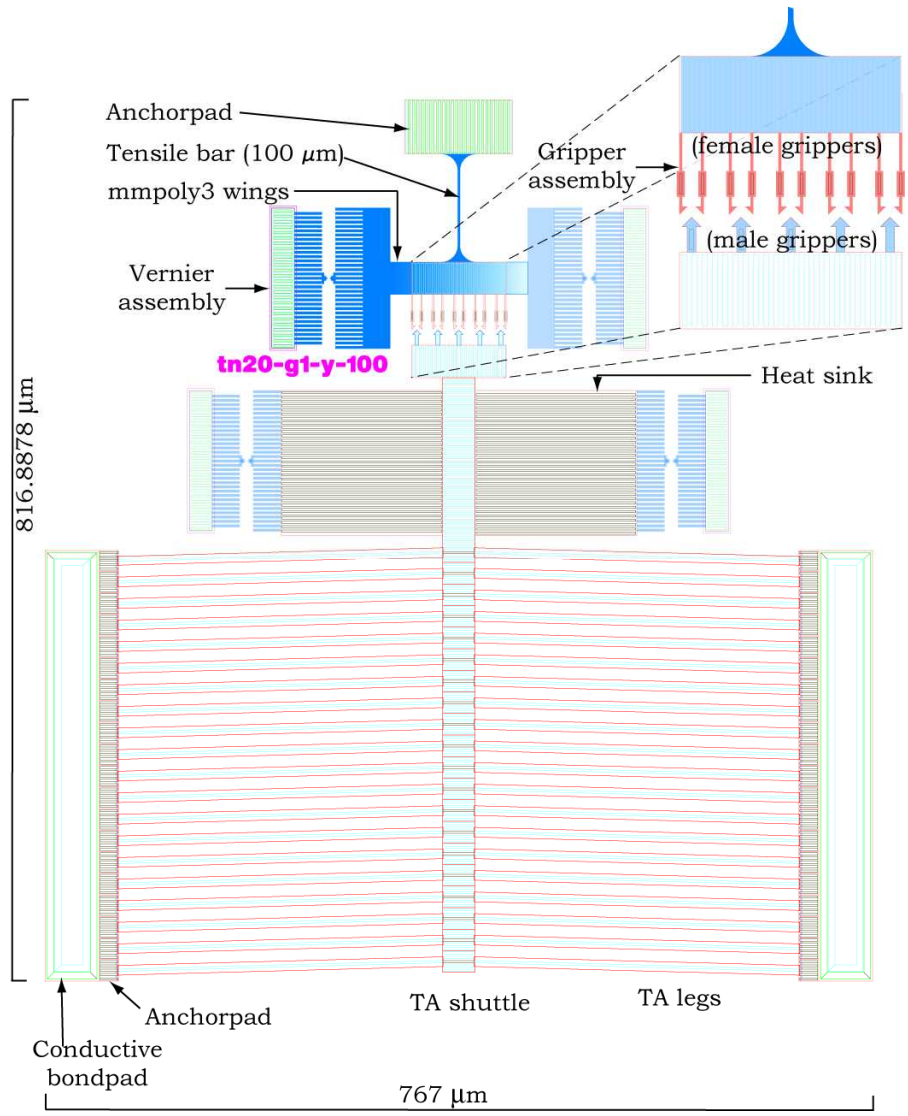


To-scale theoretical model of baseline device with 20 TA legs

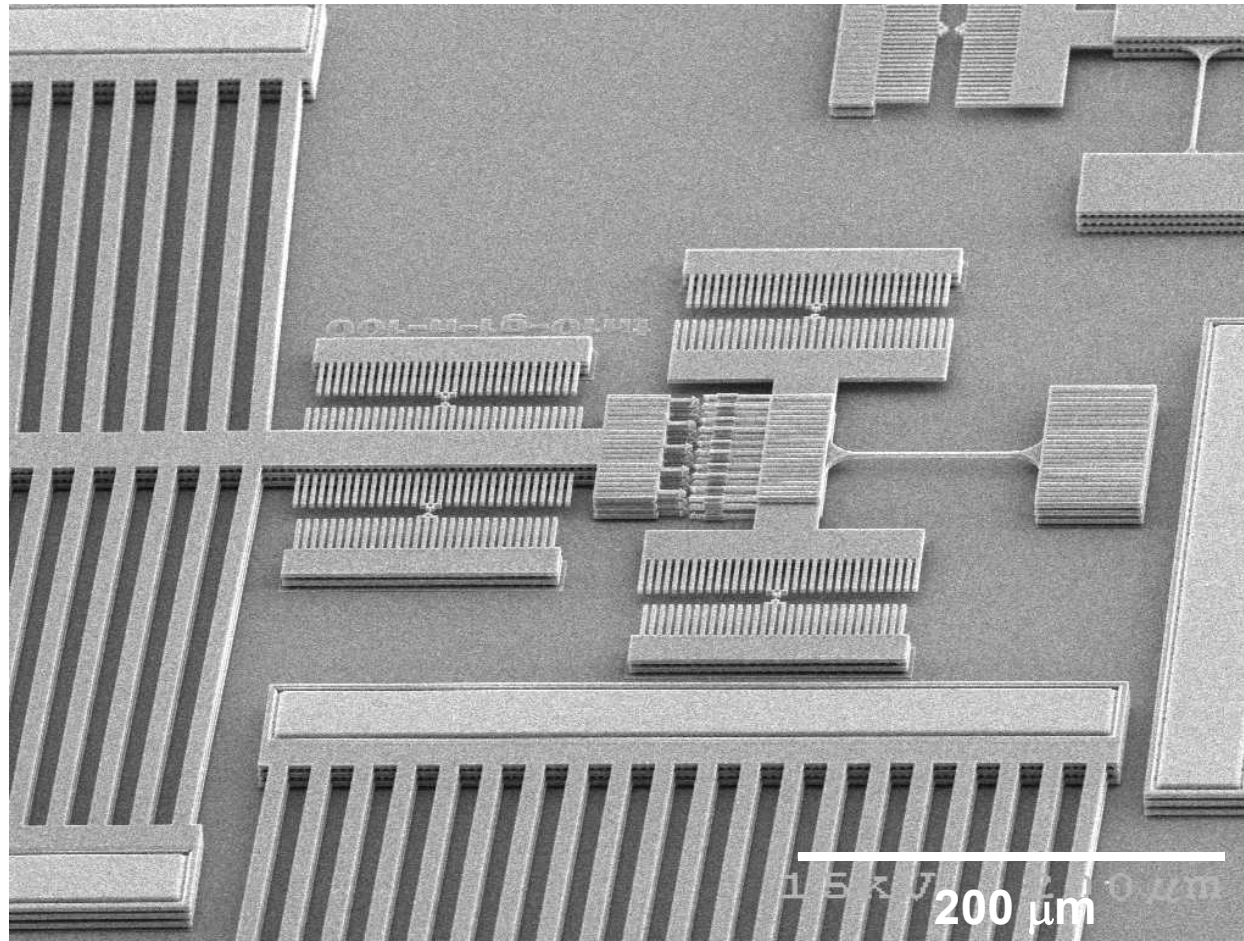


$$\frac{20 \cdot 10^{-3} \text{ N}}{4 \cdot 10^{-12} \text{ m}^2} = 5 \text{ GPa}$$

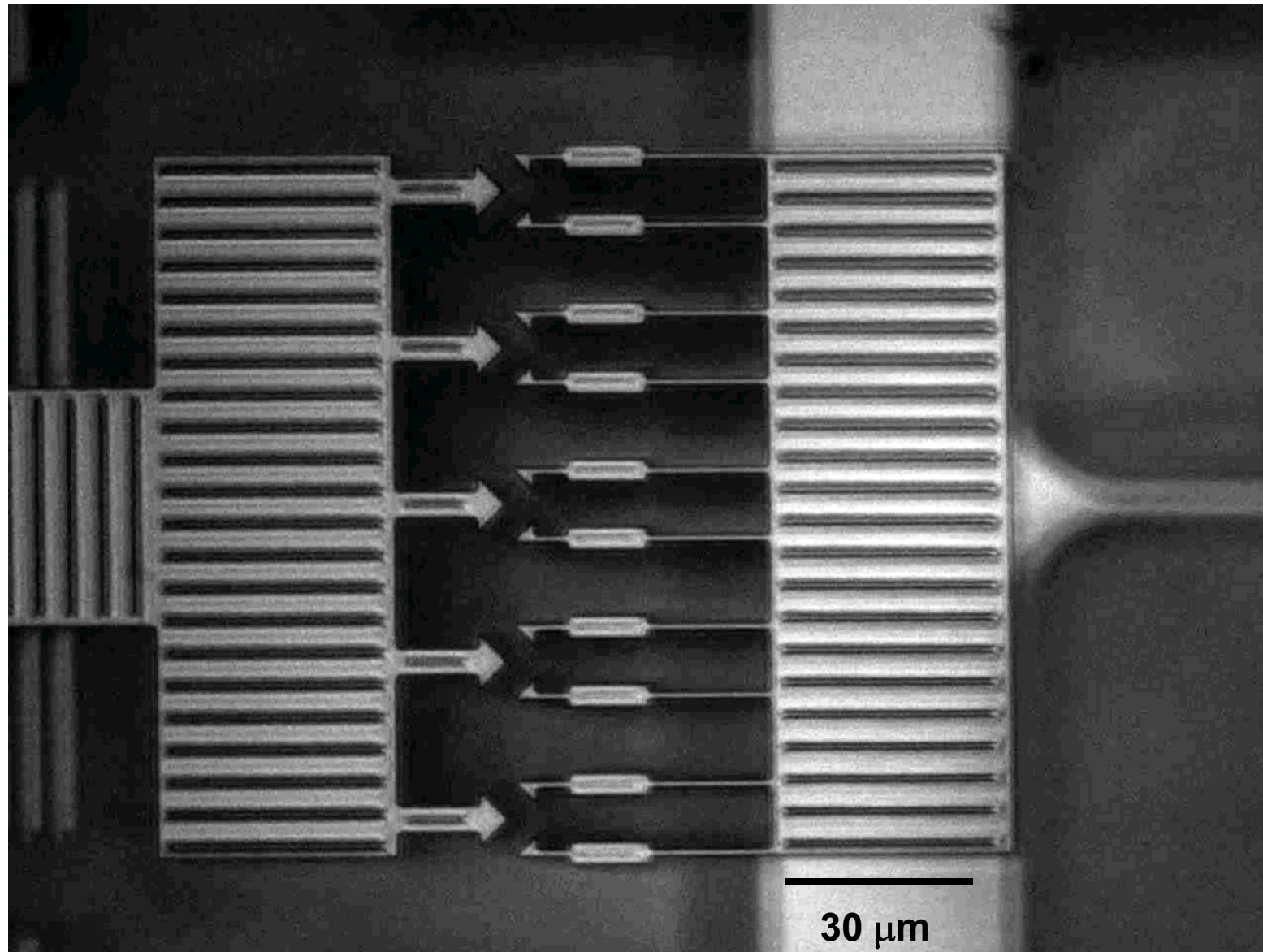
SUMMiT VTM test chip layout



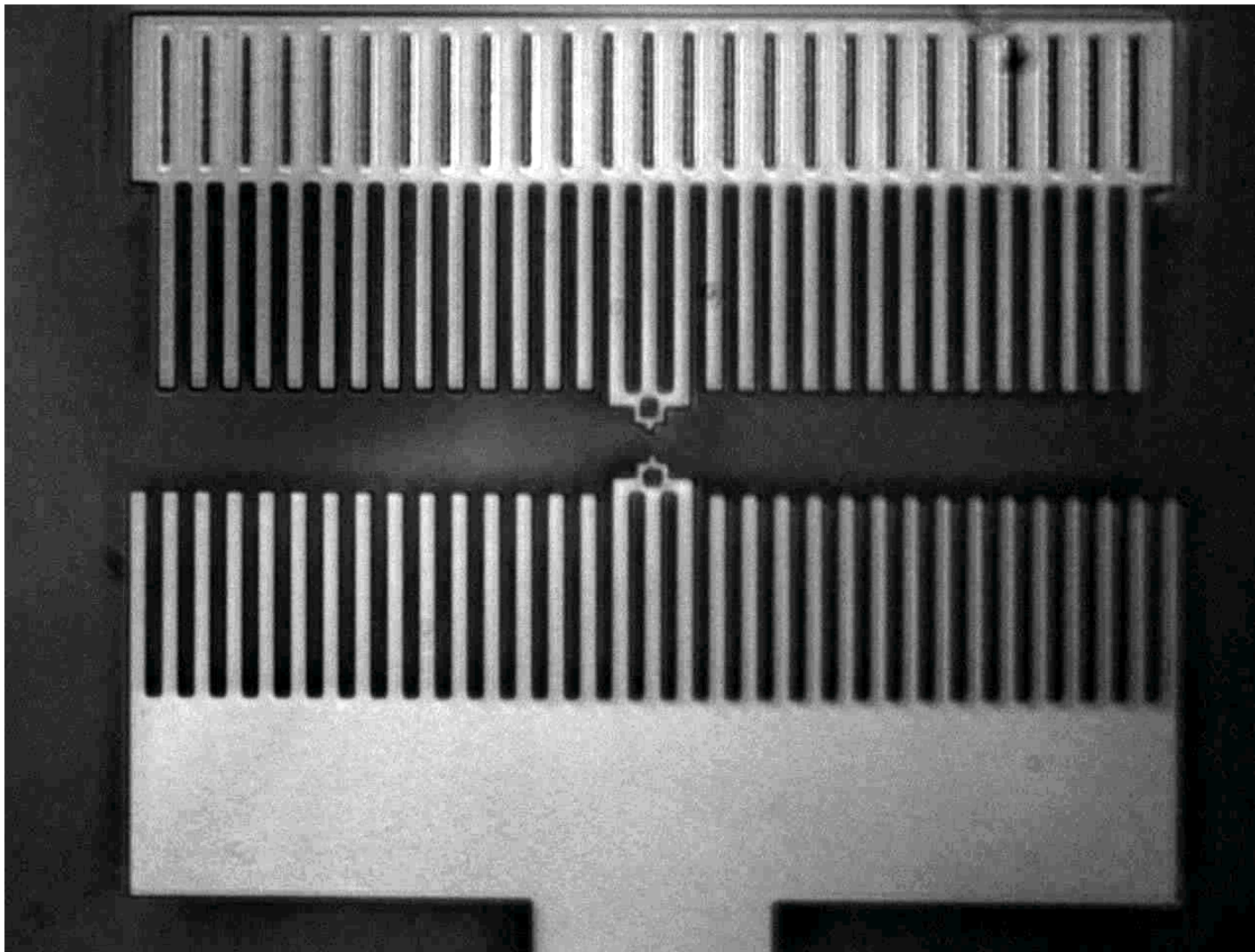
SEM image of fabricated and released device



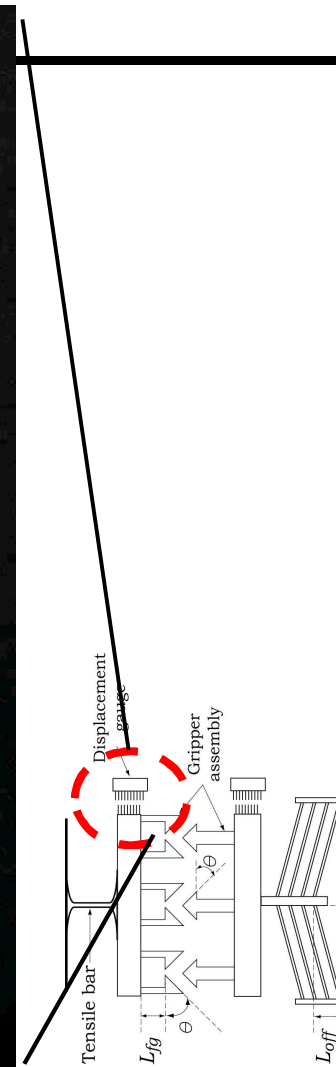
Gripper insertion movie (Optical, 50X)



Tensile-bar extension movie (Optical, 50X)

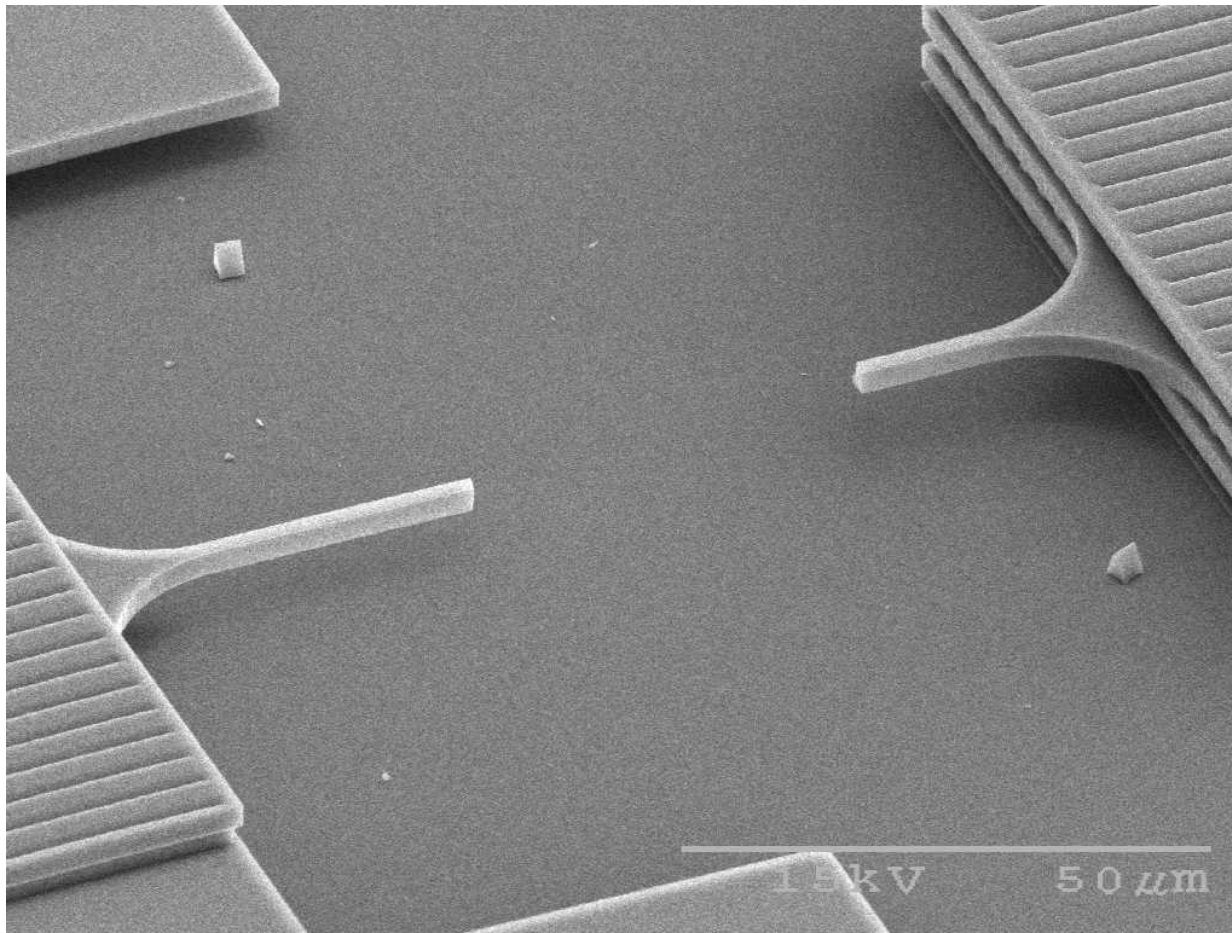


25 μm

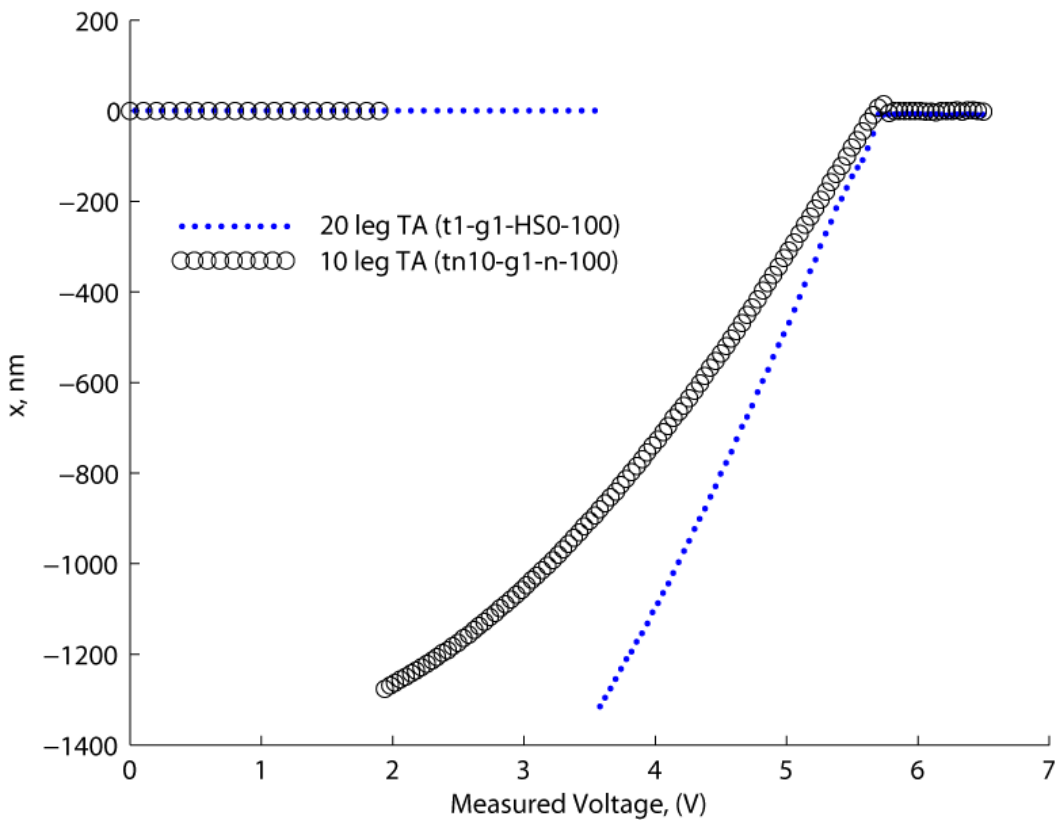


Thermal actuator $\in [3\text{mN}, 45\text{mN}]$
force output

Fractured Tensile bar



Example Data



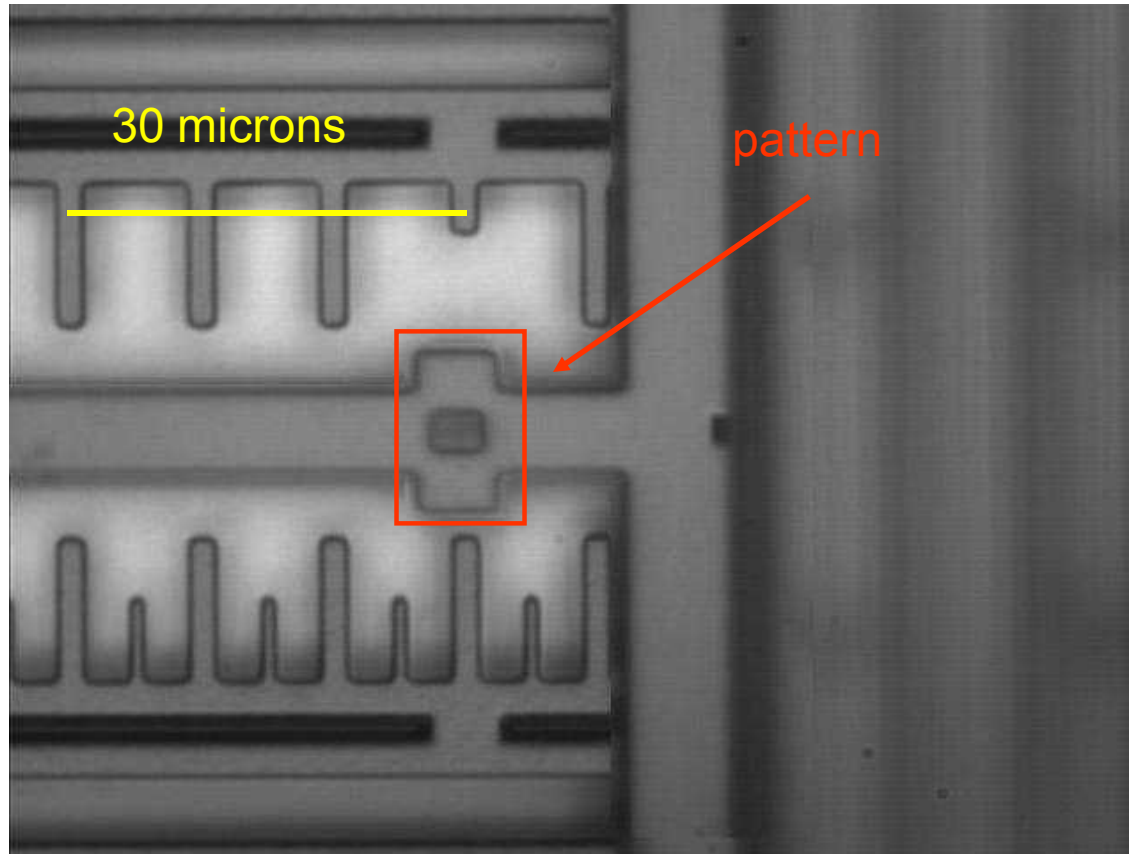
The T-bar breaks at the same displacement independent of the number of legs (validation)

Direct fracture strain measurement. Need E but not cross-sectional area to know strength

$$\sigma_f = 164 * (1.3/70) \text{ GPa} \\ = 3 \text{ GPa}$$

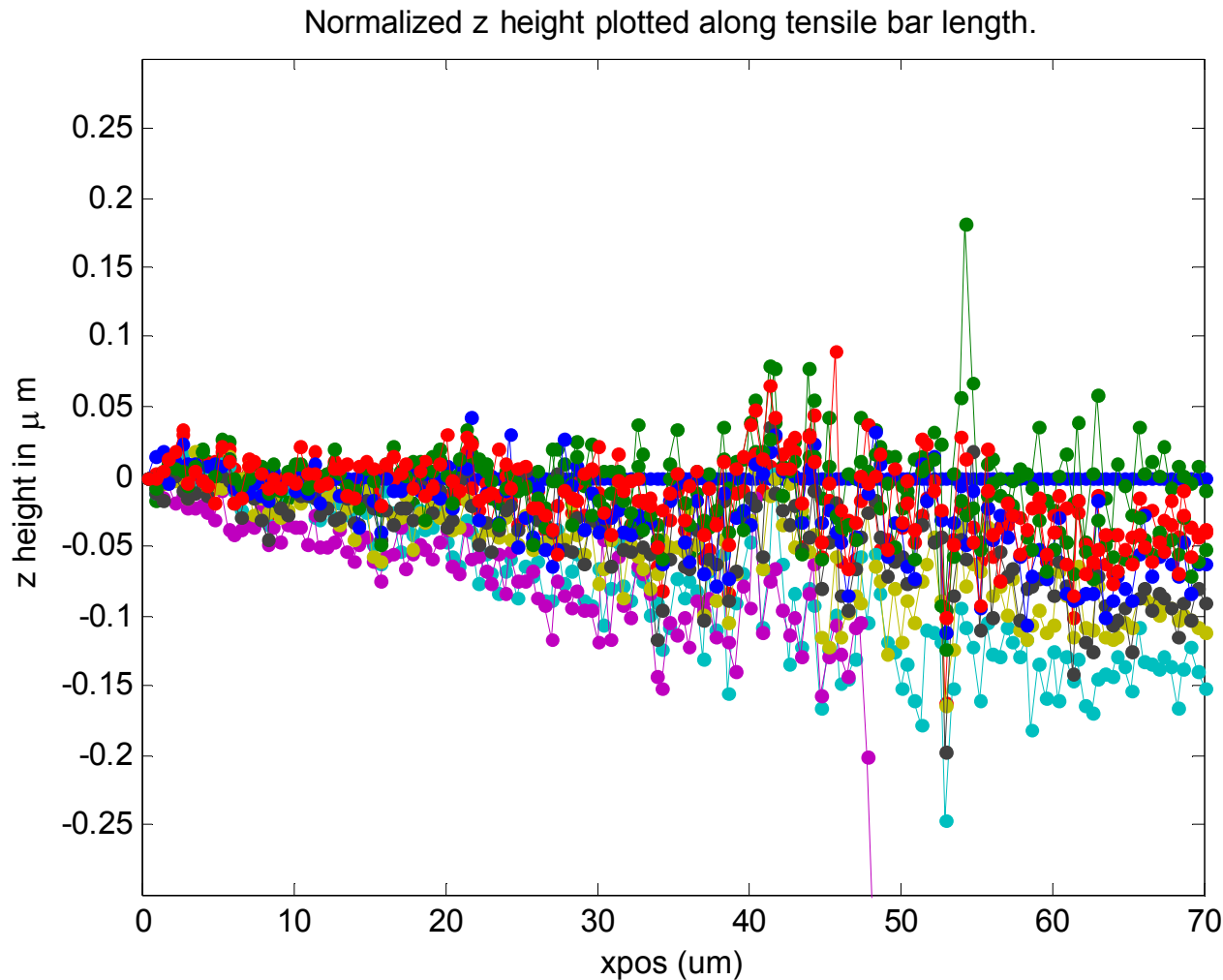
Implies no strong dependence on temperature

Optical Metrology – Pattern matching

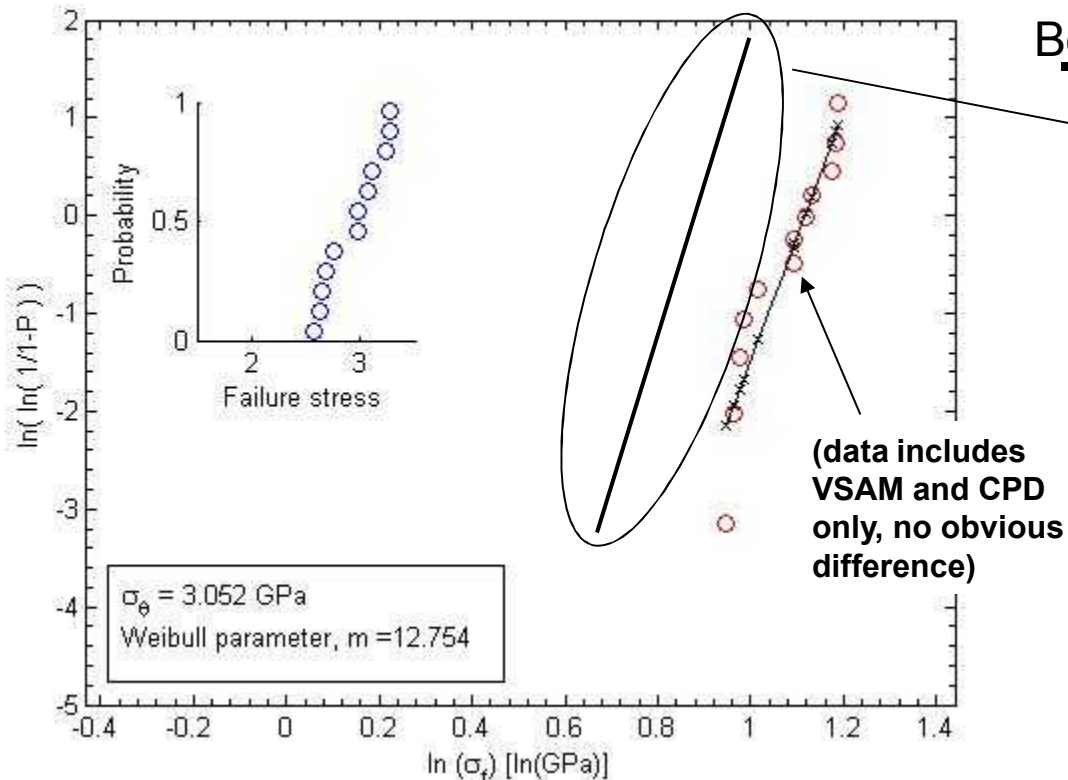


Sub-pixel pattern matching using a 50X mitutoyo objective yields ± 10 nm resolution

Out-of-plane alignment better than 0.2°



Weibull plot of 12 measurements



(data includes
VSAM and CPD
only, no obvious
difference)

Boyce (JMems, 2007)

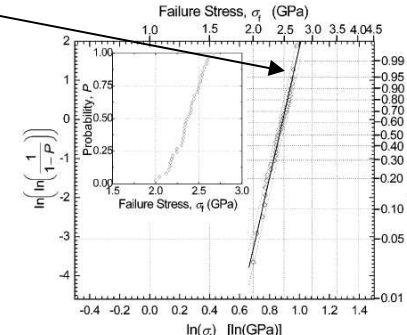
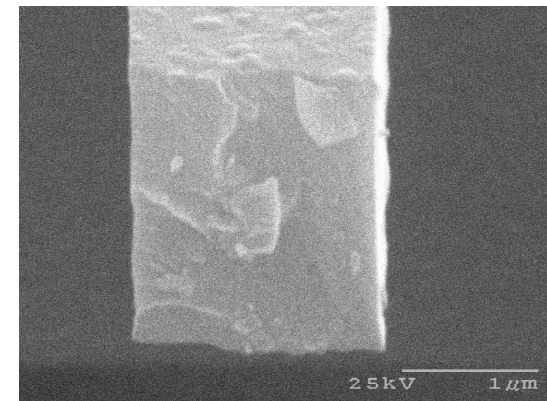


Fig. 3. The failure probability (inset) and Weibull transform observed for a unimodal strength distribution of the 150 μm long poly3 tensile structures.

$$\sigma_\theta = 2.43 \text{ GPa}$$
$$m = 16.7$$

Fracture surface

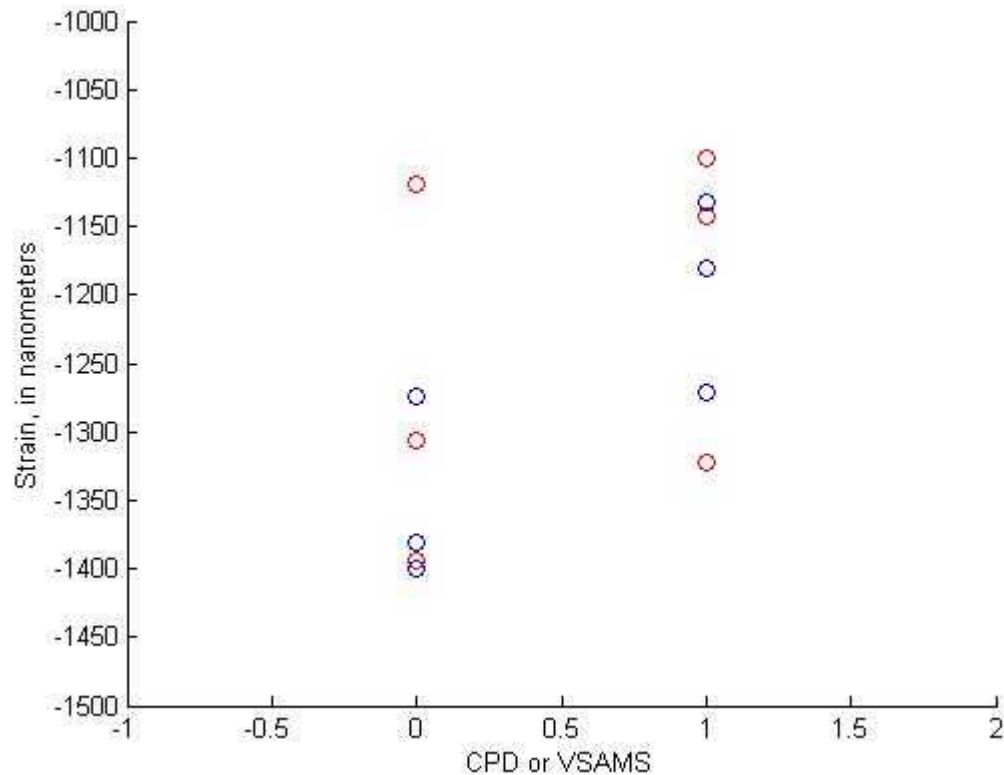


Possibly σ_θ higher because:

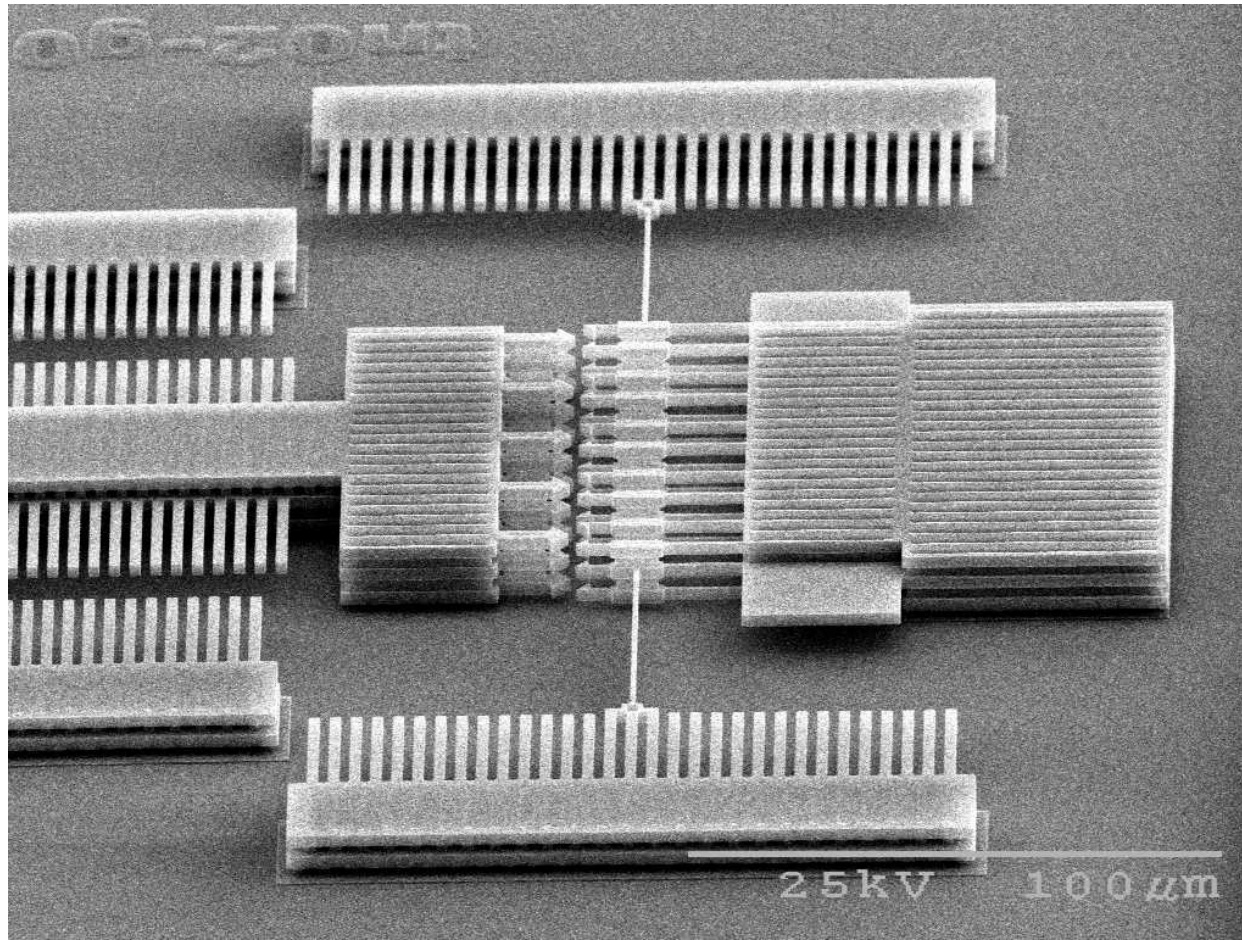
- 1) we have a direct strain measurement (would expect $(2/1.7)2.43=2.86 \text{ GPa}$ for Boyce data)
- 2) lot-to-lot dependence

S. S. Hazra, M. S. Baker, J. L. Beuth
& M. P. de Boer, J. Micromech & MicroEng (2009)

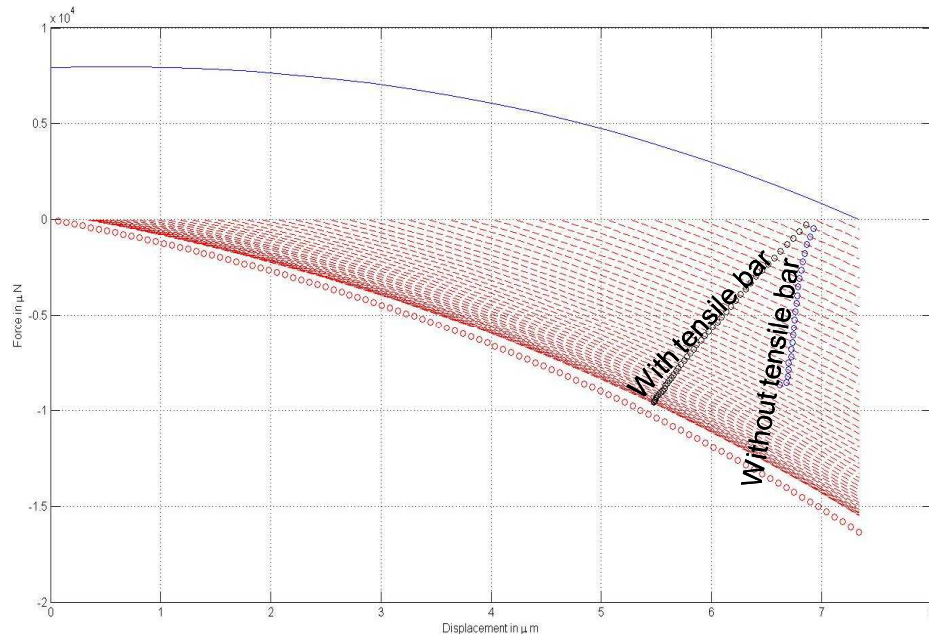
CPD vs SAMS – no apparent effect



Design with grips only (no tensile bar)



Using combined modeling and measurement approach, we can estimate gripper and T-bar compliances and hence breaking forces



Stiffness

Grips:

36627 N/m (modeled)
40000 N/m (measured)

Grips & T-bar

8987 N/m (modeled)
6818 N/m (measured)

- Red dashed lines are the structural forces at specific voltages
- Can observe “settling in” of grips only
- Measured versus estimated compliances agree relatively well! Inspires confidence in models...
- Shows that the grippers failed at lower loads for no tensile bar designs. How can this be?
- Reflects the ambiguity in defining gripper fracture (only one pair breaks which allows the rest to slip through from unbalanced forces)

Testing of brittle specimens

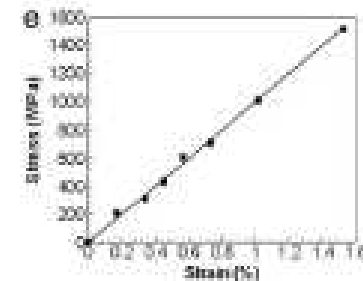
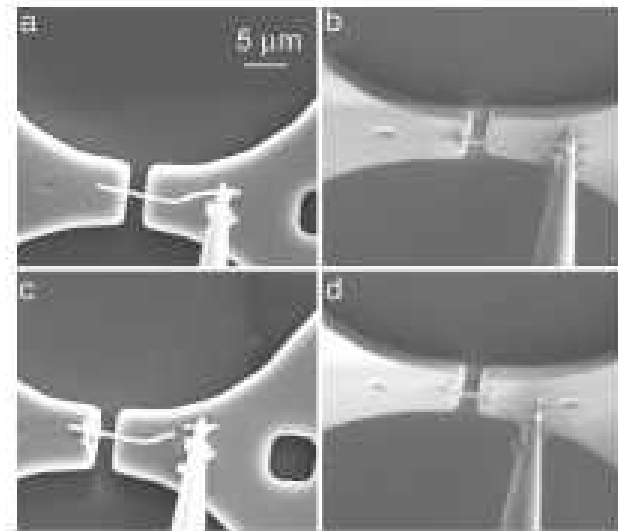
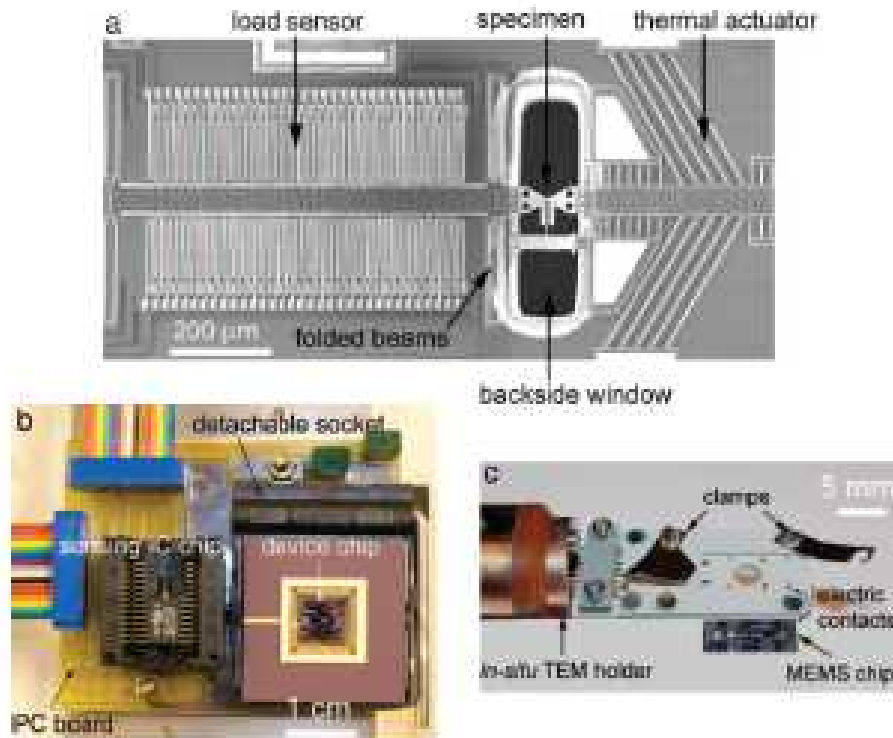
- Want to develop high forces over small displacements, but keep near room temperature
- The device concept works. Alignment is very good.
- The experiment directly measures fracture strain and fracture stress for a linear-elastic material.
- Round-robin test with Brad Boyce's pull-tab method is planned.

Nanofiber testing

An electromechanical material testing system for *in situ* electron microscopy and applications

Yong Zhu and Horacio D. Espinosa*

Department of Mechanical Engineering, Northwestern University, 2145 Sheridan Road, Evanston, IL 60208



Zhu & Espinosa (PNAS 2005)

ductile fiber testing

REVIEW OF SCIENTIFIC INSTRUMENTS 78, 085108 (2007)

Novel method for mechanical characterization of polymeric nanofibers

Mohammad Naraghi and Ioannis Chasiotis

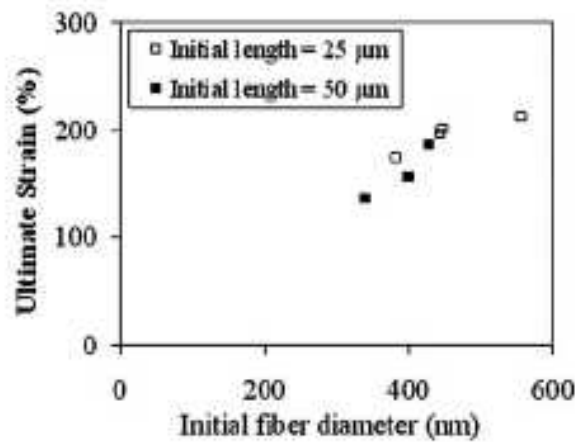
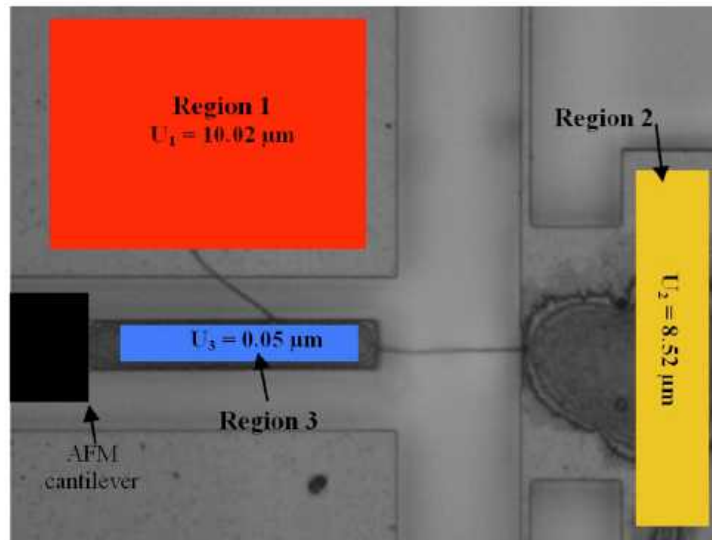
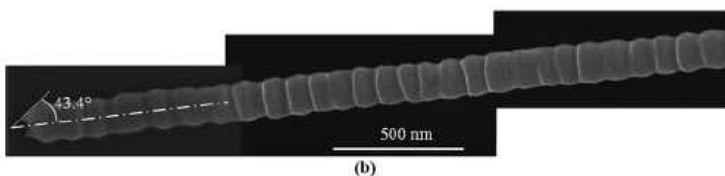
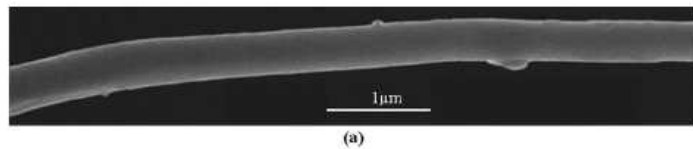
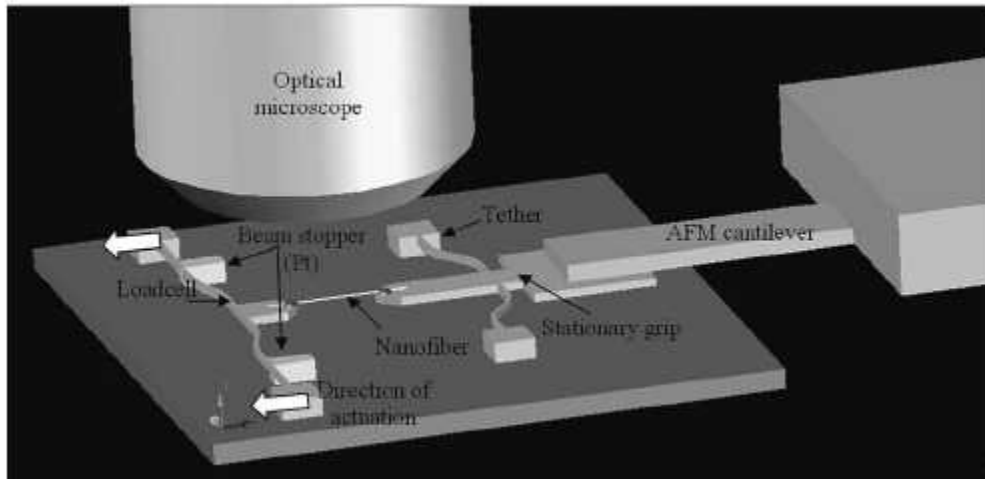
Aerospace Engineering, University of Illinois at Urbana Champaign, 325 Talbot Lab, 104 S. Wright Street, Urbana, Illinois 61801

Harold Kahn

Department of Materials Science and Engineering, Case Western Reserve University, Cleveland, Ohio 44106-7204

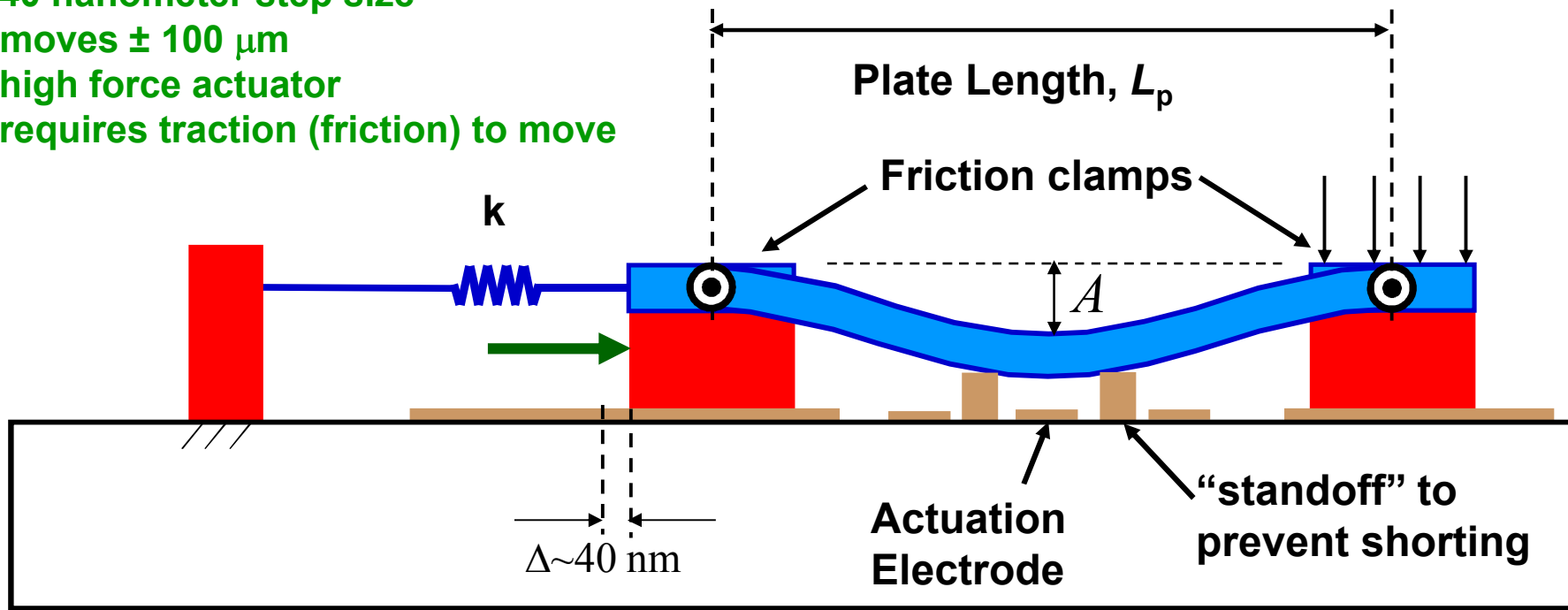
Yongkui Wen and Yuris Dzenis

Department of Engineering Mechanics, University of Nebraska, Lincoln, Nebraska 68588



ductile fiber testing – propose nanotractor for on-chip actuation

- 40 nanometer step size
- moves $\pm 100 \mu\text{m}$
- high force actuator
- requires traction (friction) to move

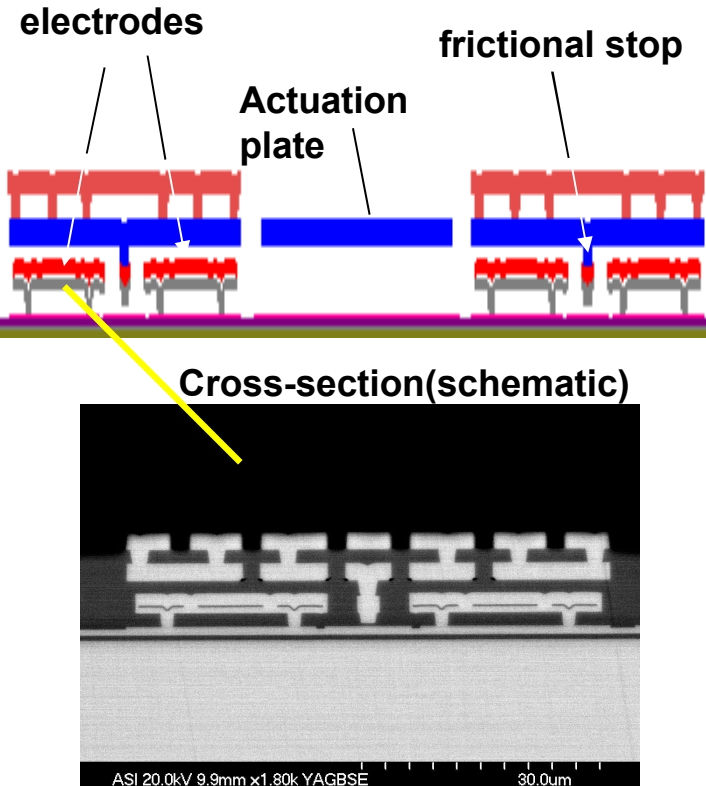
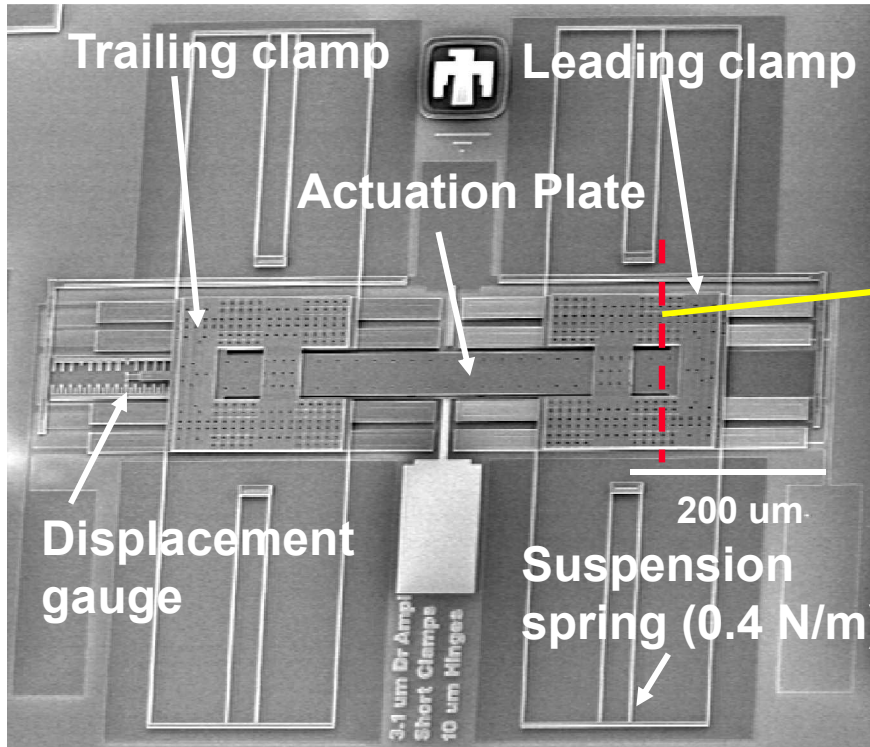


$$F_{\max} \sim 2Ewt \left(\frac{A}{L_p} \right)^2 \approx 1 \text{ mN}$$

large tangential
force range



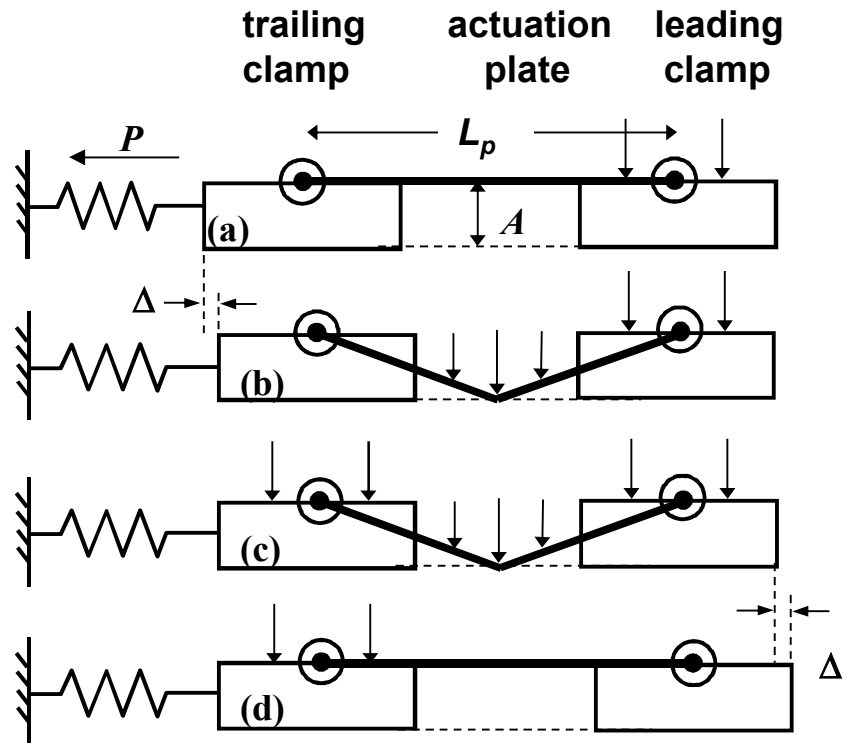
Nanotractor implementation



SEM of Friction Clamp

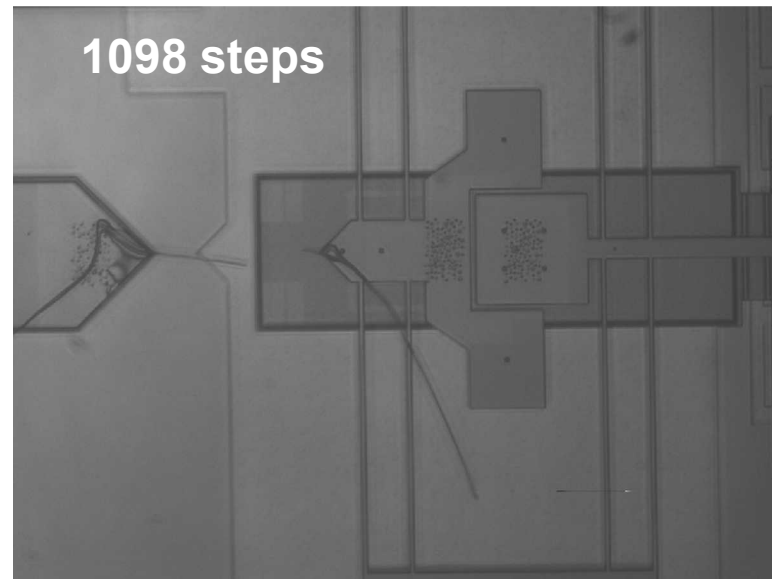
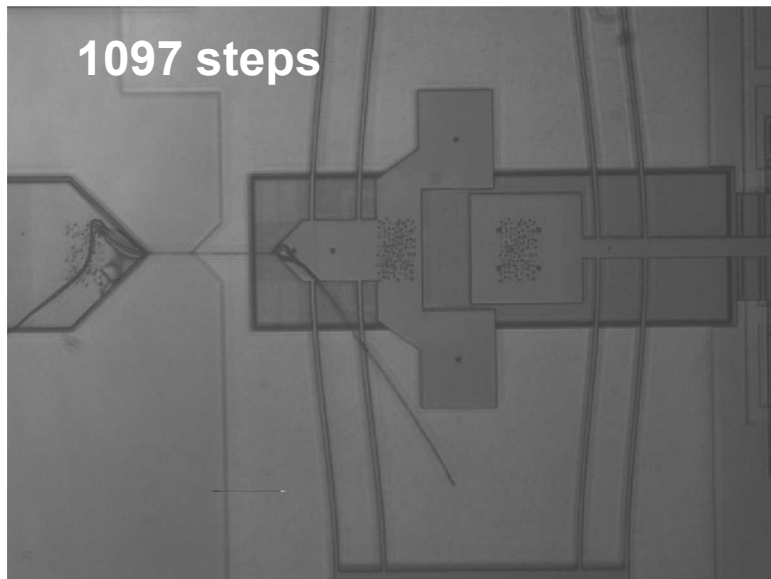
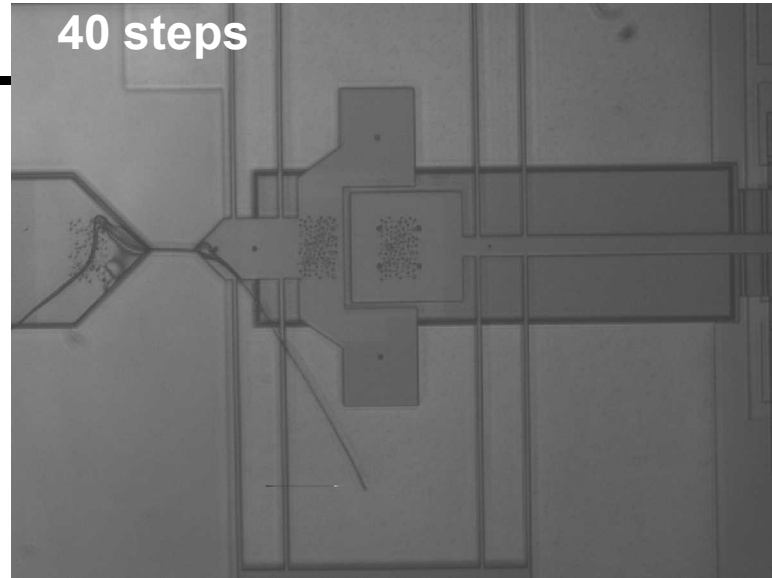
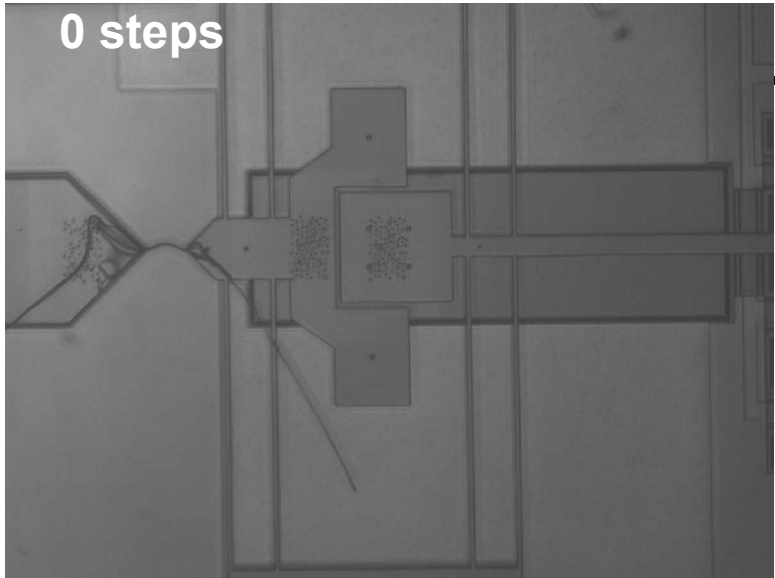
High-performance surface-micromachined inchworm actuator, de Boer, MP; Luck, DL; Ashurst, WR; Maboudian, R; Corwin, AD; Walraven, JA; Redmond, JM: *Journal of Microelectromechanical Systems*; Feb. 2004; vol.13, no.1, p.63-74

Driving the Nanotractor



- (a) Clamp RHS
- (b) Pull down driver beam
- (c) Clamp LHS
- (d) Relax RHS & driver beam

Operates up to 5 mm/s



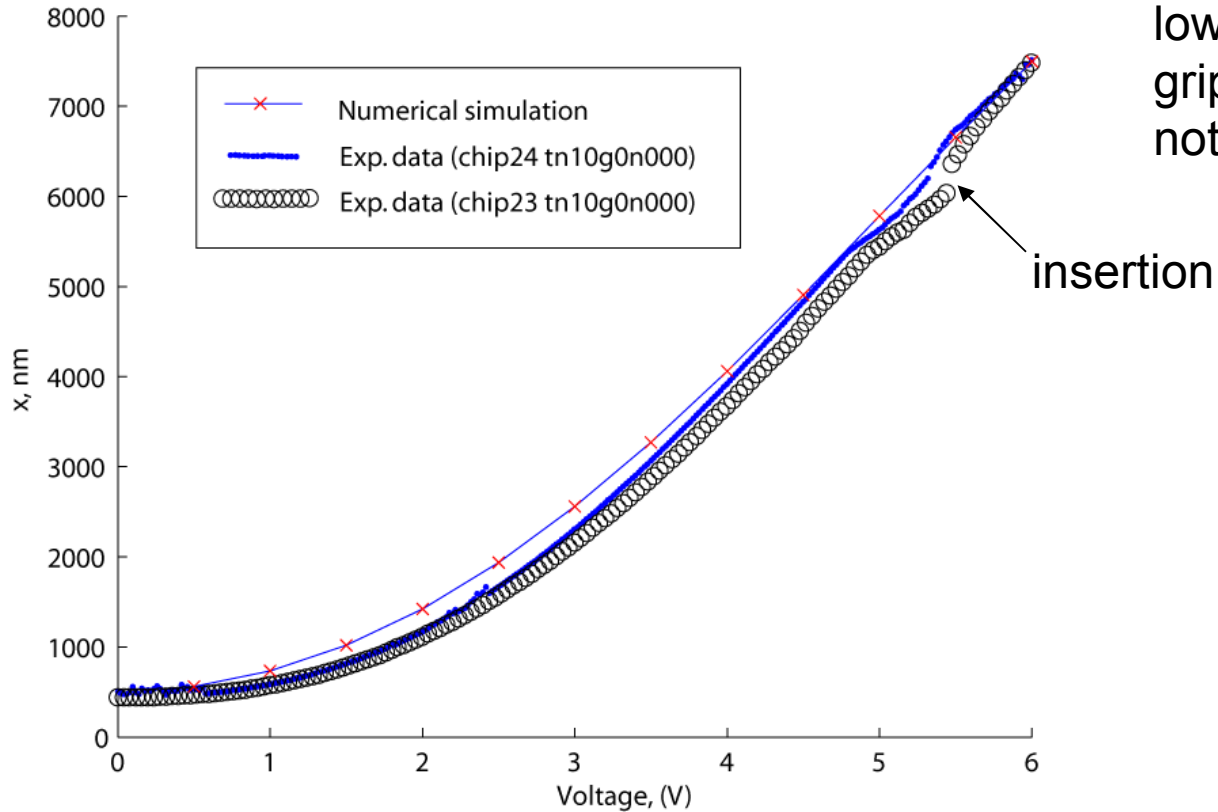
- Want to develop high forces over large displacement range
- Need only to align fiber to load spring
- Proof-of-concept shown
- Quantification possible

Closing Thoughts

In-situ nanomechanical testing:

- Samples can be adjacent to real devices
- More work to make the specimens, *but* easier to test samples and to perform a wide range of tests

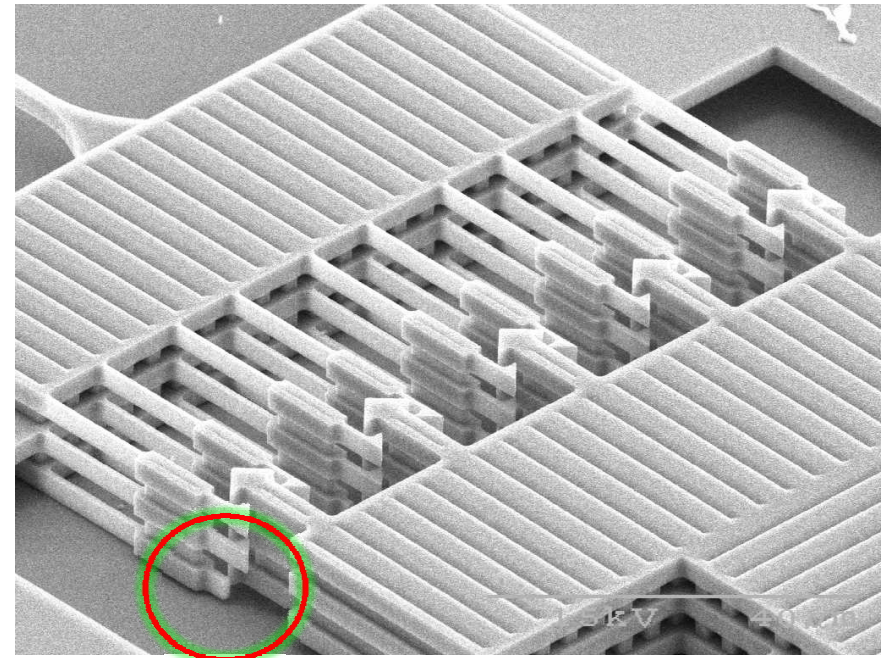
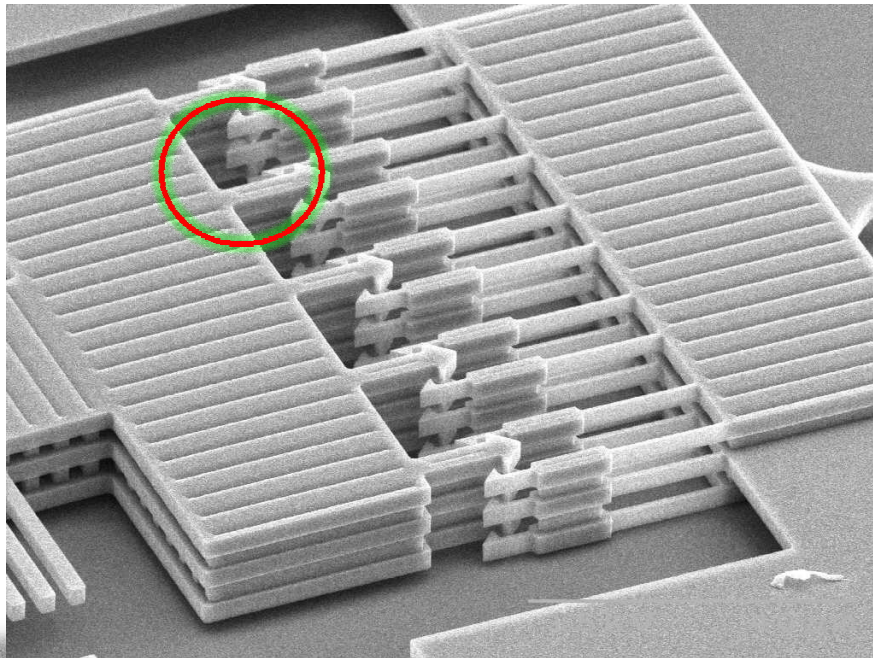
The unloaded displacement model versus measured values agree fairly well



lower breaking force of grips only is probably not due to model error.

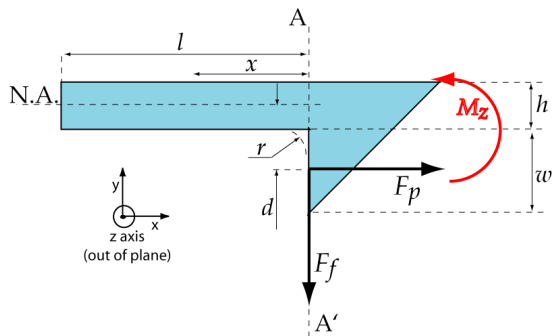
- Simulation and experimental data for insertion stage.
- Initial displacement (x @ $V=0$) is from residual stress of 10 MPa (compressive).

If the grips survive the fracture, then the results are unambiguous, but they don't... chicken or egg problem!!

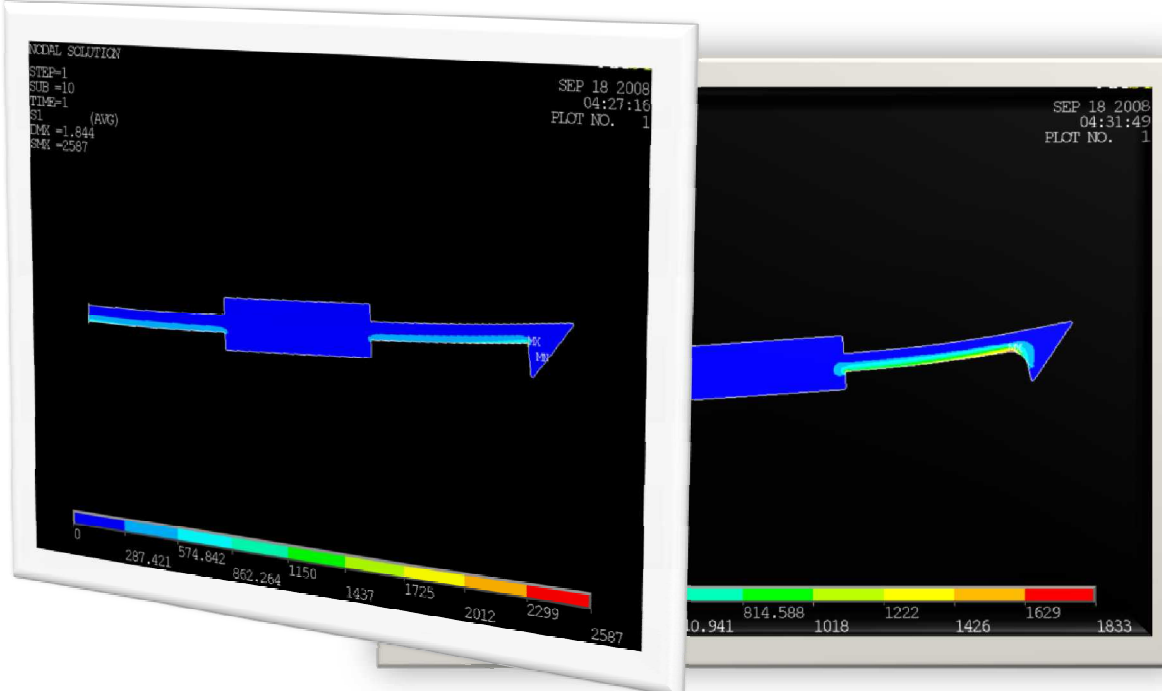
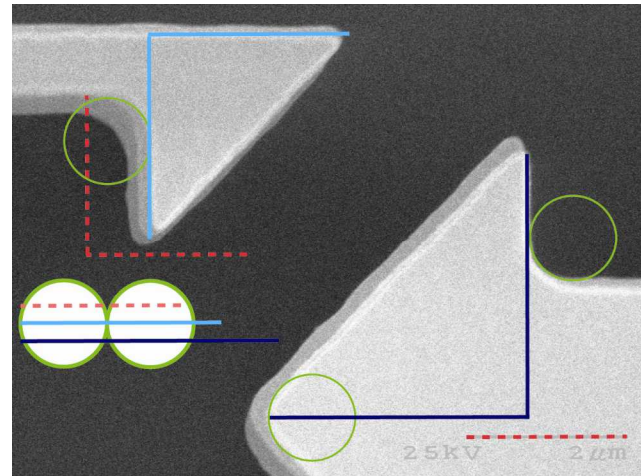


- Location of suspect broken female grips shown in red circles
- Mode of failure unknown
- Did it break before tensile specimen failed or after?
- Did it break from the normal+bending loads on the female grips or from a collision w/ ground?

We are working to estimate the gripper stresses and to redesign the gripper geometry to be more robust



- Net moment from off -centered load causes bending.
- Stress concentrated due to geom. discontinuity.



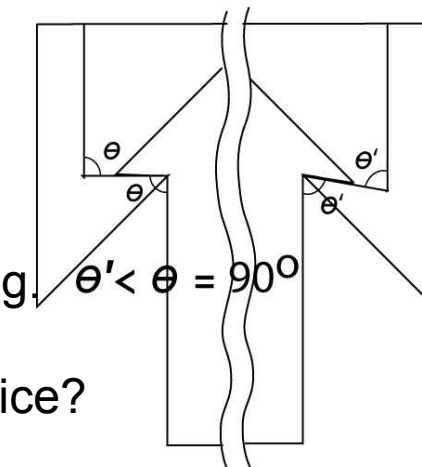
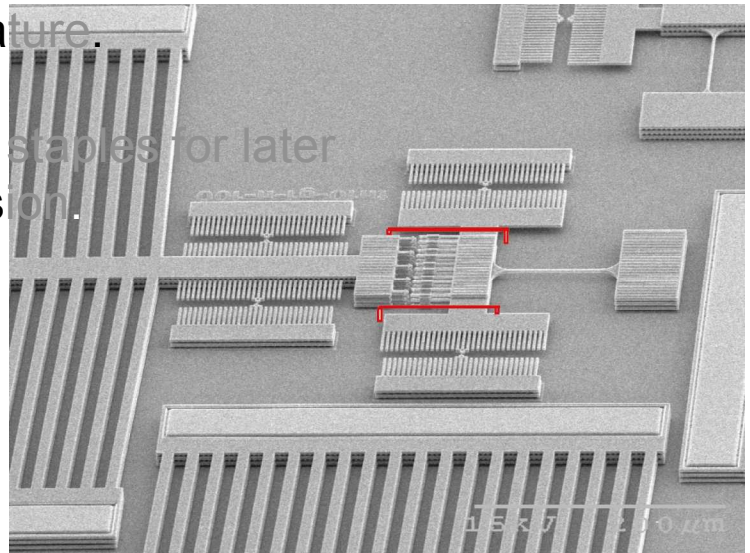
- Process induces a curvature of 0.5 μm. Max principal stress = 3 GPa
- We examine a deliberate curv. of 1 μm along with a thicker x-section; Max principal stress = 1.8 GPa (upper estimate)

- I. Device idea and design
- II. Experimental Results
- III. Future Work**
- IV. Your feedback?

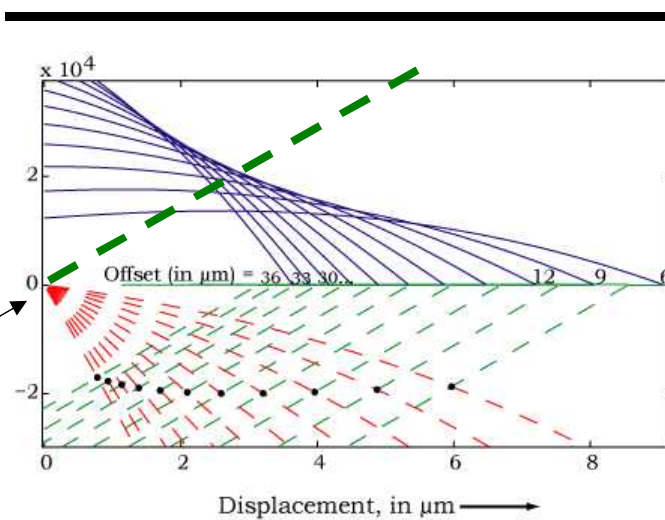
Layout variations

S.N.	TA	Grip	Mod.	Mod. val.	Heatsink	TB Length	maxDisp	Input I	Output F	Temp
1	t1MnumL	g1	numLegs	10	n	100	8.4119	177.6	12.302	603.4
2	t1MnumL	g1	numLegs	15	y	100	8.3798	266.2	16.028	600.5
3	t1MnumL	g1	numLegs	20	y	100	8.3878	355	19.068	601.3
4	t1MnumL	g1	numLegs	30 (250 w)	y	30	8.3482	532	37.042	597.78
5	t1MnumL	g1	numLegs	40	y	30	8.3878	710	45.341	601.2
6	t1Moff	g1	offset	15	y	100	6.4827	355	19.909	602.1
7	t1Moff	g1	offset	17	y	100	6.061	355	19.943	602.44
8	t1Moff	g1	offset	20	y	100	5.5086	355	19.822	603.02
9	t1	g1MnumG	numGrips	3	y	100	8.3878	355	18.958	601.3
10	t1	g1MnumG	numGrips	7	y	100	8.3878	355	19.116	601.3
11	t1	g1MnumG	numGrips/	11	y	100	8.3878	355	19.159	601.3
12	t1	g1Mthet	GD/theta	30 deg.s	y	100	8.3878	355	19.068	601.3
13	t1	g1Mthet	GD/theta	60 deg.s	y	100	8.3878	355	19.068	601.3
14	t1	g1Msxc	GD/sacOxcut	Further from grip	y	100	8.3878	355	19.068	601.3
15	t1	g1Msxc	GD/sacOxcut	No sxcuts on GD	y	100	8.3878	355	19.068	601.3
16	t1	g1	Heat sink	0 (Absent)	n	100	8.3878	355	19.068	601.3
17	t1	g1	Heat sink	Small	n	100	8.3878	355	19.068	601.3
18	t1MnumL	g1	numLegs	20	y	100	8.3878	355	19.068	601.3
19	t1MnumL	g1	numLegs	20	y	100	8.3878	355	19.068	601.3
20	t1MnumL	g0	numLegs/No TB.	10	n	0	8.4119	177.6	17.994	603.4
21	t1MnumL	g0	numLegs/No TB.	2	n	0	8.3878	35.5	3.493	601.3

1. Reduce stress concentrations on the gripper x-faces using locally thicker cross-sections and greater rad. of curvature.
2. Prevent the broken bits from flying off by using staples for later examination. Staples also prevent in-plane torsion.
3. Reduce the baseline no. of TA legs.
4. Poly2 and Poly4 tensile specimens.
5. Heat sinks with holes.
6. Length of tensile specimens.
7. Increase bond pad area.
8. Changing f-gripper x-face angle for better locking.
9. A push-device in addition to the current pull-device?



Use TA in push mode without grippers?



Loading curve for a device where fracture occurs upon pushing (heating) – TA max force about the same!

Advantage:

No grips

Disadvantages:

Fracture occurs when TA is at max temperature

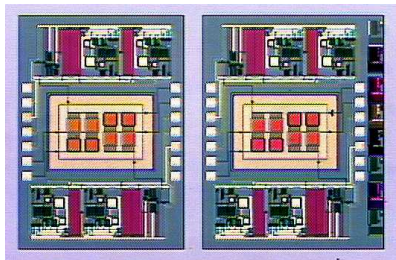
Need to account for residual stress (less absolute precision)

- **Gripper design analysis including insertion and frictional characteristics**
- **Experimental data from ~1000 devices**
- **Comparison to existing results and methods (Boyce et al., JMEMS 2007)**
- **Modeling effect of conducted heat from thermal actuator on tensile specimen and exp. results**
- **Calibration of displacement metrology**
- **Fatigue studies possible with this configuration**

MEMS are RELIABLE – Industry chooses simpler devices

Class I

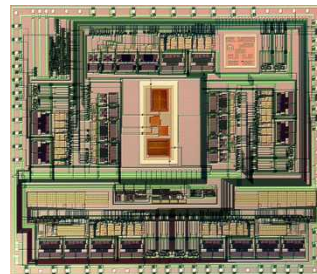
No Moving parts



Accelerometers
Pressure Sensors
Inkjet Print Heads
Strain Gauge

Class II

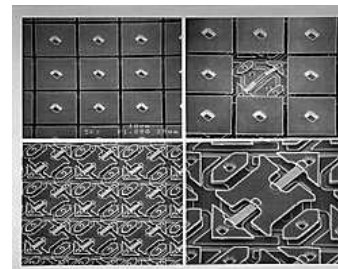
Moving Parts, No Rubbing or Impacting Surfaces



Gyros
Comb Drives
Resonators
Filters

Class III

Moving Parts, Impacting Surfaces



TI DMD (\$ 1B)
Relays
Valves
Pumps
Optical Switches

Class IV

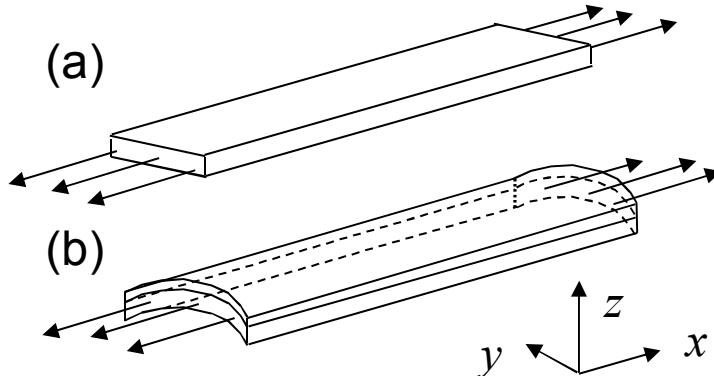
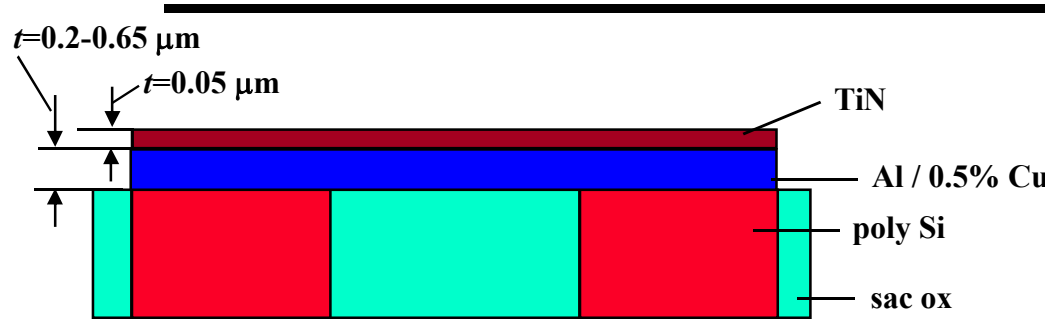
Moving Parts, Impacting and Rubbing Surfaces



Optical Switches
Shutters
Scanners
Locks
Discriminators

Billions of inkjet print cartridges produced using HP technology!
Analog Devices ships 1 million MEMS accelerometers a week!
Texas Instruments has shipped over 2 million DLP subsystems!

Sample fabrication, revisited



ff beam interferogram



100 μm

Compressive TiN protective layer induces mechanical stress relief during release

(TiN is removed after release etch)

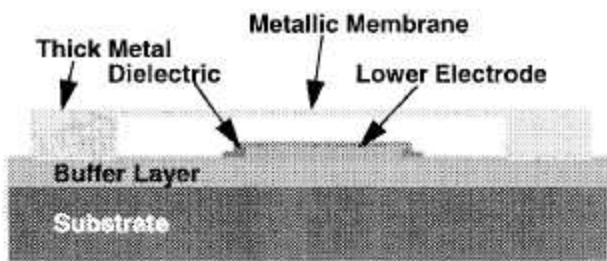


Fig. 1. Cross section of an RF MEMS capacitive switch.

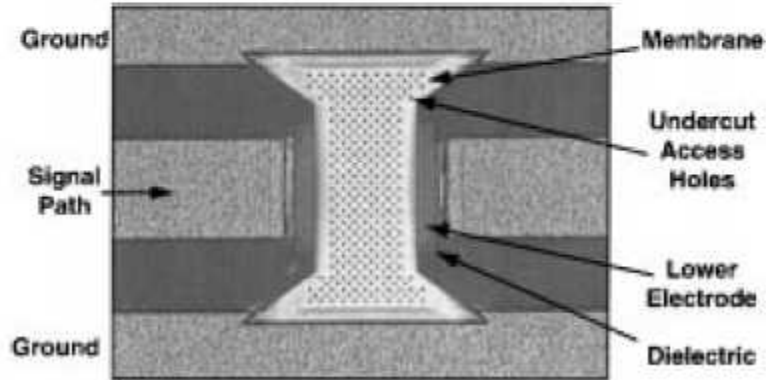
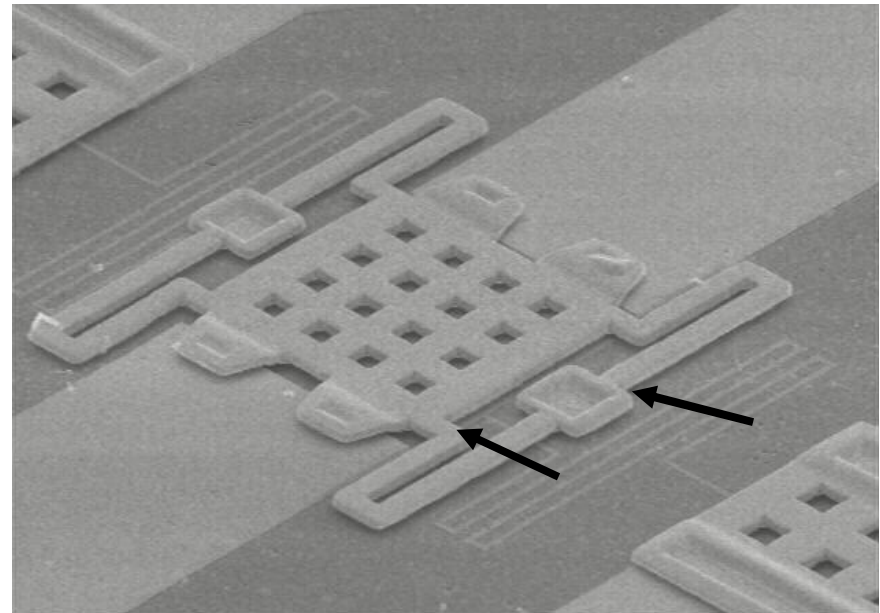


Fig. 2. Top view of a shunt MEMS capacitive switch.

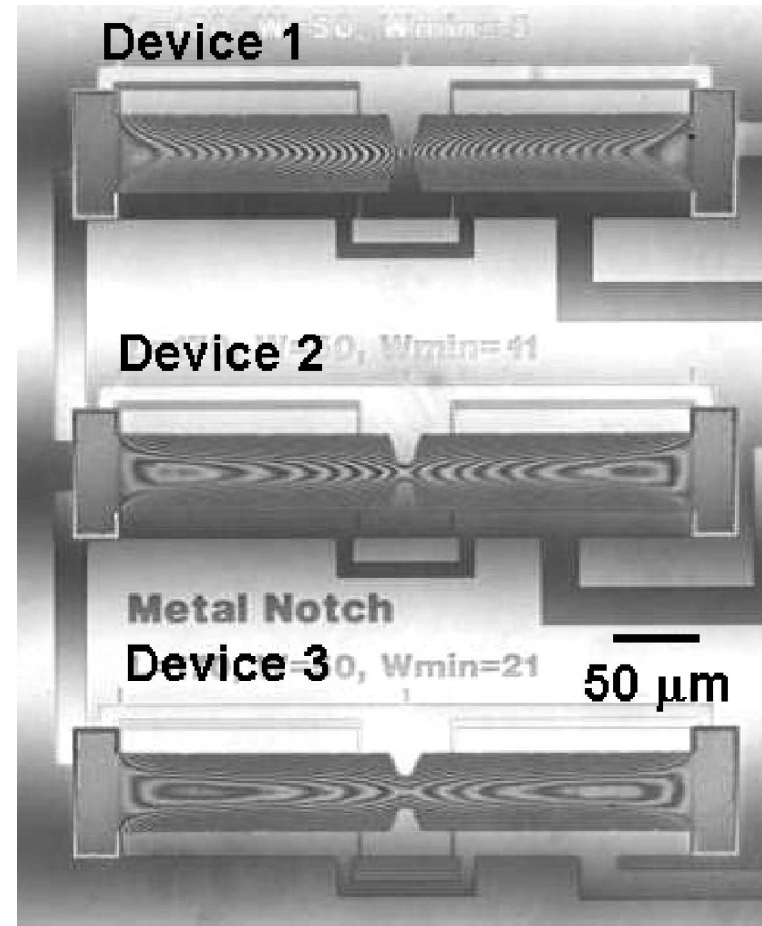
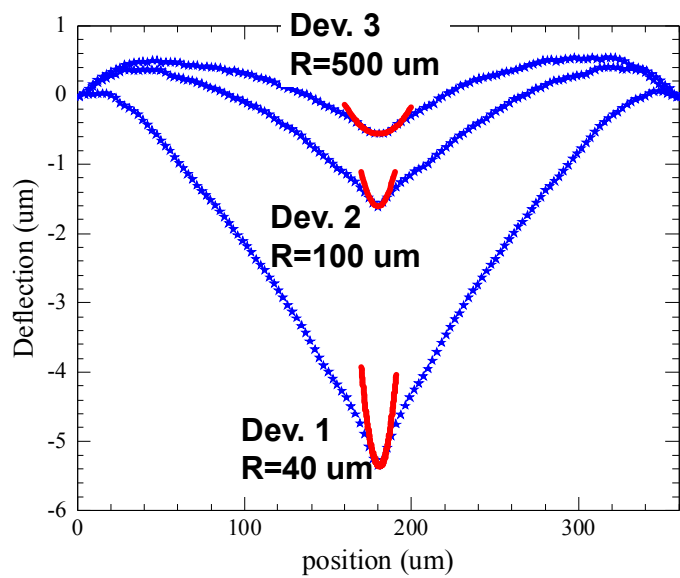


IEEE MICROWAVE AND GUIDED WAVE LETTERS, VOL. 8, NO. 8, AUGUST 1998

Performance of Low-Loss RF MEMS Capacitive Switches

Charles L. Goldsmith, *Senior Member, IEEE*, Zhimin Yao, *Member, IEEE*,
Susan Eshelman, *Member, IEEE*, and David Denniston, *Member, IEEE*

TiN also induces arc lengthening in the notched devices, stretching the gage section in Devices 1& 2



Assess the Young's Modulus with a cantilever geometry

Assess the needs

Design & Model Test Structures

Fabricate

Test

Analyze and compare to model

Look at course outline to see what can be incorporated